

Deep Learning for Neuroimaging-based Diagnosis and Rehabilitation of Autism Spectrum Disorder: A Review

Marjane Khodatars, Afshin Shoeibi, Delaram Sadeghi, Navid Ghassemi, Mahboobeh Jafari, Parisa Moridian, Ali Khadem, Roohallah Alizadehsani, Assef Zare, Yinan Kong, Abbas Khosravi, Saeid Nahavandi, Sadiq Hussain, U. Rajendra Acharya, Michael Berk

Abstract—Accurate diagnosis of Autism Spectrum Disorder (ASD) followed by effective rehabilitation is essential for the management of this disorder. Artificial intelligence (AI) techniques can aid physicians to apply automatic diagnosis and rehabilitation procedures. AI techniques comprise traditional machine learning (ML) approaches and deep learning (DL) techniques. Conventional ML methods employ various feature extraction and classification techniques, but in DL, the process of feature extraction and classification is accomplished intelligently and integrally. DL methods for diagnosis of ASD have been focused on neuroimaging-based approaches. Neuroimaging techniques are non-invasive disease markers potentially useful for ASD diagnosis. Structural and functional neuroimaging techniques provide physicians substantial information about the structure (anatomy and structural connectivity) and function (activity and functional connectivity) of the brain. Due to the intricate structure and function of the brain, proposing optimum procedures for ASD diagnosis with neuroimaging data without exploiting powerful AI techniques like DL may be challenging. In this paper, studies conducted with the aid of DL networks to distinguish ASD are investigated. Rehabilitation tools provided for supporting ASD patients utilizing DL networks are also assessed. Finally, we will

present important challenges in the automated detection and rehabilitation of ASD and propose some future works.

Index Terms—Autism Spectrum Disorder, Diagnosis, Rehabilitation, Deep Learning, Neuroimaging, Neuroscience.

I. INTRODUCTION

ASD is a disorder of the nervous system that affects the brain and results in difficulties in speech, social interaction and communication deficits, repetitive behaviors, and delays in motor abilities [1]. This disease can generally be distinguished with extant diagnostic protocols from the age of three years onwards. Autism influences many parts of the brain. This disorder also involves a genetic influence via the gene interactions or polymorphisms [2], [3]. One in 70 children worldwide is affected by autism. In 2018, the prevalence of ASD was estimated to occur in 168 out of 10,000 children in the United States, one of the highest prevalence rates worldwide. Autism is significantly more common in boys than in girls. In the United States, about 3.63 percent of boys aged 3 to 17 years have autism spectrum disorder, compared with approximately 1.25 percent of girls [4].

Diagnosing ASD is difficult because there is no pathophysiological marker, relying instead just on psychological criteria [5]. Psychological tools can identify individual behaviors, levels of social interaction, and consequently facilitate early diagnosis. Behavioral evaluations embrace various instruments and questionnaires to assist the physicians to specify the particular type of delay in a child's development, including clinical observations, medical history, autism diagnosis instructions, and growth and intelligence tests [6].

Several investigations for the diagnosis of ASD have recently been conducted on neuroimaging data (structural and functional).

Analyzing anatomy and structural connections of brain areas with structural neuroimaging is an essential tool for studying structural disorders of the brain in ASD. The principal tools for structural brain imaging are magnetic resonance imaging (MRI) techniques [7], [8], [9]. Cerebral anatomy is investigated by structural MRI (sMRI) images and anatomical connections are assessed by diffusion tensor imaging MRI (DTI-MR) [10]. Investigating the activity and functional connections of brain areas using functional neuroimaging can also be used for studying ASD. Brain functional diagnostic

M. Khodatars and D. Sadeghi are with the Dept. of Medical Engineering, Mashhad Branch, Islamic Azad University, Mashhad, Iran.

A. Shoeibi and N. Ghassemi are with the Faculty of Electrical Engineering, FPGA Lab, K. N. Toosi University of Technology, Tehran, Iran, and the Computer Engineering Department, Ferdowsi University of Mashhad, Mashhad, Iran. (Corresponding author: Afshin Shoeibi, email: afshin.shoeibi@gmail.com).

M. Jafari is with Electrical and Computer Engineering Faculty, Semnan University, Semnan, Iran.

P. Moridian is with the Faculty of Engineering, Science and Research Branch, Islamic Azad University, Tehran, Iran.

A. Khadem is with the Faculty of Electrical Engineering, K. N. Toosi University of Technology, Tehran, Iran. (Corresponding author: Ali Khadem, email: alikhadem@kntu.ac.ir).

R. Alizadehsani, A. Khosravi and S. Nahavandi. are with the Institute for Intelligent Systems Research and Innovation (IISRI), Deakin University, Victoria 3217, Australia.

A. Zare is with Faculty of Electrical Engineering, Gonabad Branch, Islamic Azad University, Gonabad, Iran.

Y. Kong is with the School of Engineering, Macquarie University, Sydney, 2109, Australia.

S. Hussain is with the Dibrugarh University, Assam, India, 786004.

U. R. Acharya is with the Dept. of Electronics and Computer Engineering, Ngee Ann Polytechnic, Singapore 599489, Singapore, the Dept. of Biomedical Informatics and Medical Engineering, Asia University, Taichung, Taiwan, and the Dept. of Biomedical Engineering, School of Science and Technology, Singapore University of Social Sciences, Singapore.

M. Berk is with the Deakin University, IMPACT - the Institute for Mental and Physical Health and Clinical Translation, School of Medicine, Barwon Health, Geelong, Australia, and the Orygen, The National Centre of Excellence in Youth Mental Health, Centre for Youth Mental Health, Florey Institute for Neuroscience and Mental Health and the Department of Psychiatry, The University of Melbourne, Melbourne, Australia.

tools are older approaches than structural methods for studying ASD. The most basic modality of functional neuroimaging is electroencephalography (EEG), which records the electrical activity of the brain from the scalp with a high temporal resolution (in milliseconds order) [11]. Studies have shown that employing EEG signals to diagnose ASD have been useful [12], [13], [14]. Functional MRI (fMRI) is one of the most promising imaging modalities in functional brain disorders, used as task-based (T-fMRI) or resting-state (rs-fMRI) [15], [16]. fMRI-based techniques have a high spatial resolution (in the order of millimeters) but a low temporal resolution due to slow response of the hemodynamic system of the brain as well as fMRI imaging time constraints and is not ideal for recording the fast dynamics of brain activities. In addition, these techniques have a high sensitivity to motion artifacts. It should be stressed that in consonance with studies, three less prevalent modalities of electrocorticography (ECoG) [17], functional near-infrared spectroscopy (fNIRS) [18], and Magnetoencephalography (MEG) [19] can also attain reasonable performance in ASD diagnosis. An appropriate approach is to utilize machine-learning techniques alongside functional and structural data to collaborate with physicians in the process of accurately assessing ASD. In the field of ASD, applying machine learning methods generally entail two categories of traditional methods [20] and DL methods [21]. As opposed to traditional methods, much less work has been done on DL methods to explore ASD or design rehabilitation tools.

This study reviews ASD assessment methods and patients' rehabilitation with DL networks. The outline of this paper is as follows. Section 2 is search strategy. Section 3 concisely presents the DL networks employed in the field of ASD. In section 4, existing computer-aided diagnosis systems (CADs) that use brain functional and structural data are reviewed. In section 5, DL-based rehabilitation tools for supporting ASD patients are introduced. Section 6 discusses the reviewed papers. Section 7 reveals the challenges of ASD diagnosis and rehabilitation with DL. Finally, the paper concludes and suggests future work in section 8.

II. SEARCH STRATEGY

In this review, IEEE Xplore, ScienceDirect, SpringerLink, ACM, as well as other conferences or journals were used to acquire papers on ASD diagnosis and rehabilitation using DL methods. Further, the keywords "ASD", "Autism Spectrum Disorder" and "Deep Learning" were used to select the papers. The papers are analyzed till June 03th, 2020 by the authors (AK, SN). Figure 1 depicts the number of considered papers using DL methods for the automated detection and rehabilitation of ASD each year.

III. DEEP LEARNING TECHNIQUES FOR ASD DIAGNOSIS AND REHABILITATION

Nowadays, DL algorithms are used in many areas of medicine including structural and functional neuroimaging. The application of DL in neural imaging ranges from brain MR image segmentation [22], to detection of brain lesions such as tumors [23], diagnosis of brain functional disorders

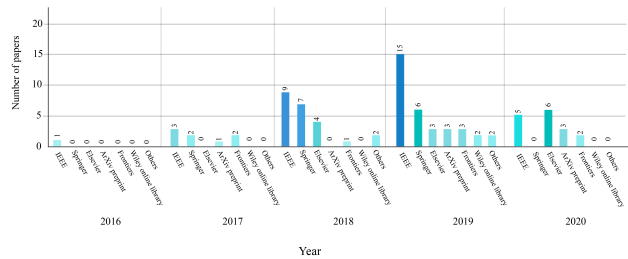


Fig. 1: Number of papers published every year for ASD diagnosis and rehabilitation.

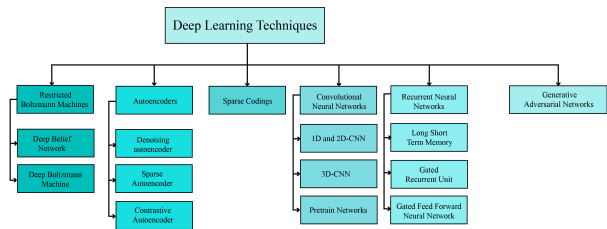


Fig. 2: Illustration of various types of DL methods.

such as ASD [24], and production of artificial structural or functional brain images [25]. Machine learning techniques are categorized into three fundamental categories of learning: supervised learning [26], unsupervised learning [27], and reinforcement learning [28], and a variety of DL networks are provided for each type. So far, most studies applied to identify ASD using DL have been based on supervised or unsupervised approaches. Figure 2 illustrates generally employed types of DL networks with supervised or unsupervised learning to study ASD.

IV. CADs-BASED DEEP LEARNING TECHNIQUES FOR ASD DIAGNOSIS BY NEUROIMAGING DATA

A traditional artificial intelligence (AI)-based CADs encompasses several stages of data acquisition, data pre-processing, feature extraction, and classification [29], [30], [31], [32]. In [33], [34], [35] existing traditional algorithms for diagnosing ASD have been reviewed. In contrast to traditional methods, in DL-based CADs, feature extraction, and classification are performed intelligently within the model. Also, due to the structure of DL networks, using large dataset to train DL networks and recognize intricate patterns in datasets is incumbent. The components of DL-based CADs for ASD detection are shown in Figure 3. It can be noted from the figure that, large and free databases are first introduced to diagnose ASD. In the second step, various types of pre-processing techniques are used on functional and structural data to be scrutinized. Finally, the DL networks are applied on the preprocessed data.

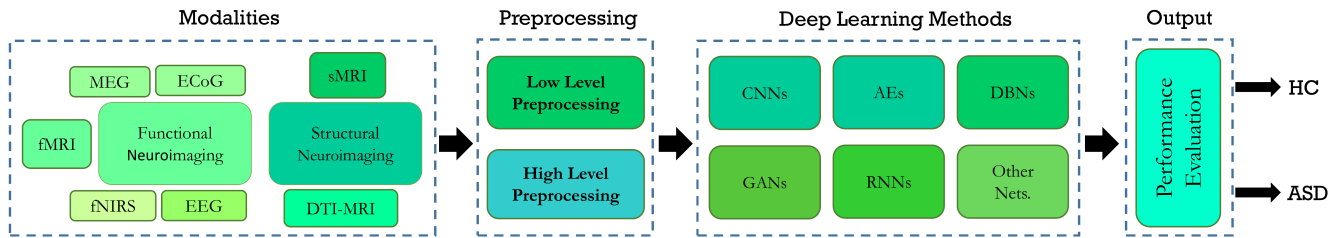


Fig. 3: Block diagram of CAD system using DL architecture for ASD detection.

A. Neuroimaging ASD Datasets

Datasets are the heart of any CADs development and the capability of CADs depends primarily on the affluence of the input data. To diagnose ASD, several brain functional and structural datasets are available. The most complete free dataset available is ABIDE [36] dataset with two subsets: ABIDE-I and ABIDE-II, which encompasses sMRI, rs-fMRI, and phenotypic data. ABIDE-I involves data from 17 international sites, yielding a total of 1112 datasets, including 539 individuals with ASD and 573 healthy individuals (ages 64-7). In accordance with HIPAA guidelines and 1000 FCP / INDI protocols, these data are anonymized. In contrast, ABIDE-II contains data from 19 international sites, with a total of 1114 datasets from 521 individuals with ASD and 593 healthy individuals (ages 5-64). Also, preprocessed images of the ABIDE-I series called PCP [37] can be freely downloaded by the researchers. The second recently released ASD diagnostic database is called NDAR, which comprises various modalities, and more information is provided in [38].

B. Preprocessing Techniques

Neuroimaging data (especially functional ones) is of relatively complicated structure, and if not pre-processed properly, it may affect the final diagnosis. Preprocessing of this data typically entails multiple common steps performed by different software as standard. Indeed, occasionally prepared pipelines are applied on the dataset to yield pre-processed data for future researchers. In the following section, preprocessing steps are briefly explained for fMRI data.

1) *Standard (Low-level) fMRI preprocessing steps:* Low-level pre-processing of fMRI images normally has fixed number of steps applied on the data, and prepared toolboxes are usually used to reduce execution time and yield better accuracy. Some of these reputable toolboxes contain FMRIB software libraries (FSL) [39], BET [40], FreeSurfer [41], and SPM [42]. Also, important and vital fMRI preprocessing incorporates brain extraction, spatial smoothing, temporal filtering, motion correction, slice timing correction, intensity normalization, and registration to standard atlas, which are summarized as follows:

BRAIN EXTRACTION: the goal is to remove the skull and cerebellum from the fMRI image and maintain the brain tissue [43], [44], [45].

SPATIAL SMOOTHING: involves averaging the adjacent voxels signal. This process is persuasive on account of neighbor-

ing brain voxels being usually closely related in function and blood supply [43], [44], [45].

TEMPORAL FILTERING: the aim is to eliminate unwanted components from the time series of voxels without impairing the signal of interest [43], [44], [45].

REALIGNMENT (MOTION CORRECTION): During the fMRI test, people often move their heads. The objective of motion correction is to align all images to a reference image so that the coordinates and orientation of the voxels be identical in all fMRI volumetric images [43], [44], [45].

SLICE TIMING CORRECTION: The purpose of modifying the slice time is to adjust the time series of the voxels so that all the voxels in each fMRI volume image have a common reference time. Usually, the corresponding time of the first slice recorded in each fMRI volume image is selected as the reference time [43], [44], [45].

INTENSITY NORMALIZATION: at this stage, the average intensity of fMRI signals are rescaled to compensate for global deviations within and between the recording sessions [43], [44], [45].

REGISTRATION TO A STANDARD ATLAS: The human brain entails hundreds of cortical and subcortical areas with various structures and functions, each of which is very time-consuming and complex to study. To overcome the problem, brain atlases are employed to partition brain images into a confined number of ROIs, following which the mean time series of each ROI can be extracted [46]. ABIDE datasets use a manifold of atlases, including Automated Anatomical Labeling (AAL) [47], Eickhoff-Zilles (EZ) [48], Harvard-Oxford (HO) [49], Talarach and Tournoux (TT) [50], Dosenbach 160 [51], Craddock 200 (CC200) [52] and Craddock 400 (CC400) [53] and more information is provided in [54]. Table I provides complete information on preprocessing tools, atlases, and some other preprocessing information.

2) *Pipeline Methods:* Pipelines present preprocessed images of ABIDE databases. They embrace generic preprocessing procedures. Employing pipelines, distinct methods can be compared with each other. In ABIDE datasets, preprocessing is performed by four pipeline techniques: neuroimaging analysis kit (NIAK) [55], data processing assistant for rs-fMRI (DPARF) [56], the configurable pipeline for the analysis of connectomes (CPAC) [57], or connectome computation system (CCS) [58]. The preprocessing steps carried out by the various pipelines are comparatively analogous. The chief differences are in the particular algorithms for each step, the software simulations, and the parameters applied. Details of each pipeline technique are provided in [54]. Table I

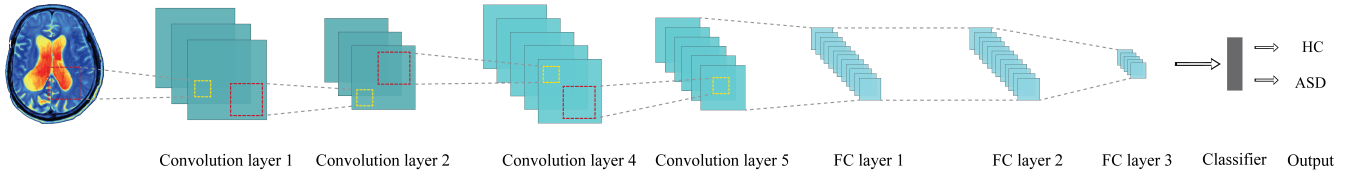


Fig. 4: Overall block diagram of a 2D-CNN used for ASD detection.

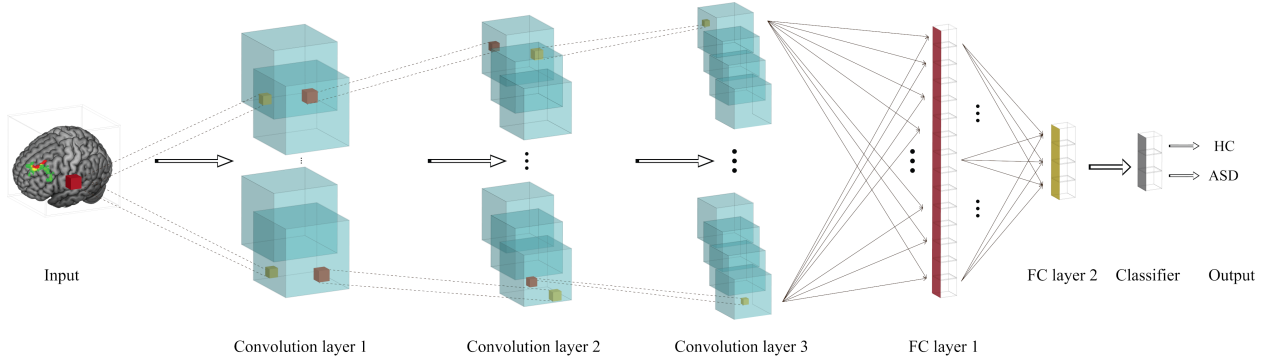


Fig. 5: Overall block diagram of a 3D-CNN used for ASD detection.

demonstrates the pipeline techniques used in autism detection exploiting DL.

3) *High-level preprocessing Steps*: High-level techniques for pre-processing brain data are important, and using them accompanying preliminary pre-processing methods can enhance the accuracy of ASD recognition. These methods are applied after the standard pre-processing of functional and structural brain data. These include sliding window (SW) [24], data augmentation (DA) [59], functional connectivity matrix (FCM) estimation [60], [61] and applying fast Fourier transformation (FFT) [62]. Furthermore, some of the researches utilized feature extraction [63] techniques and some also use feature selection methods. Precise information on reviewed studies is indicated in detail in Table I.

C. Deep Neural Networks

Deep learning in various medical applications, including the diagnosis of ASD, has become extremely popular in recent years. In this section of the paper, the types of Deep Learning networks used in ASD detection are examined, which include CNN, RNN, AE, DBN, CNN-RNN, and CNN-AE models.

1) *Convolutional Neural Networks (CNNs)*: In this section, the types of popular convolutional networks used in ASD diagnosis are surveyed. These networks involve 1D-CNN, 2D-CNN, 3D-CNN models, and a variety of pre-trained networks such as VGG.

1D AND 2D-CNN

There are many spatial dependencies present in the data and it is difficult to extract these hidden signatures from the data. Convolution network uses a structure alike to convolution filters to extract these features properly and contribute to the knowledge that features should be processed taking into account spatial dependencies; so the number of network parameters are significantly reduced. The principal application of these networks is in image processing and due to the

two-dimensional (2D) image inputs, convolution layers form 2D structures, which is why these networks are called 2D convolutional neural network (2D-CNN). By using another type of data, one-dimensional signals, the convolution layers' structure also resembles the data structure [64]. In convolution networks, assuming that various data sections do not require learning different filters, the number of parameters are markedly lessened and make it feasible to train these networks with smaller databases [21]. Figure 4 shows the block diagram of 2D-CNN used for ASD detection.

3D-CNN

By transforming the data into three dimensions, the convolution network will also be altered to a three-dimensional format (Figure 5). It should be noted that the manipulation of three dimensional CNN (3D-CNN) networks is less beneficial than 1D-CNN and 2D-CNN networks for diverse reasons. First, the data required to train these networks must be much larger which conventionally such datasets are not utilizable and methods such as pre-training, which are extensively exploited in 2D networks, cannot be used here. Another reason is that with more complicated structure of networks, it becomes much tougher to fix the number of layers, and network structure. The 3D activation map generated during the convolution of a 3D CNN is essential for analyzing data where volumetric or temporal context is crucial. This ability to analyze a series of frames or images in context has led to the use of 3D CNNs as tools for action detection and evaluation of medical imaging. [65].

2) *Deep Belief Networks (DBNs)*: DBNs are not popular today as they used to be, and have been substituted by new models to perform various applications (e.g., autoencoders for unsupervised learning, generative adversarial networks (GAN) for generative modes [66], variational autoencoders (VAE) [67]). However, disregarding the restricted use of these networks in this era, their influence on the advancement of neural

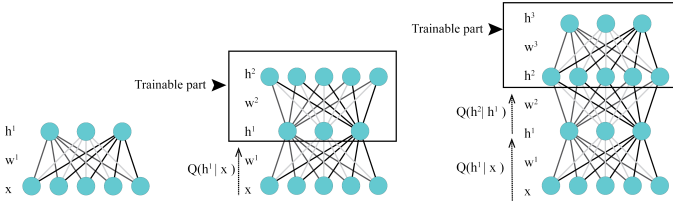


Fig. 6: Overall block diagram of a DBN used for ASD detection.

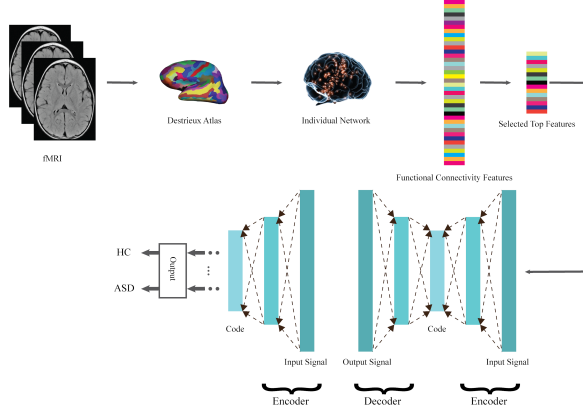


Fig. 7: Overall block diagram of an AE used for ASD detection.

networks cannot be overlooked. The use of these networks in this paper is related to the feature extraction without a supervisor or pre-training of networks. These networks serve as unsupervised, consisting of several layers after the input layer, which are shown in Figure 6. The training of these networks is done greedily and from bottom to top, in other words, each separate layer is trained and then the next layer is appended. After training, these networks are used as a feature extractor or the network weights are used as initial weights of a network for classification [21].

3) *Autoencoders (AEs)*: Autoencoders (AEs) are more than 30 years old, and have undergone dramatic changes over the years to enhance their performance. But the overall structure of these networks has remained the same [21]. These networks consist of two parts: coder and decoder so that the first part of the input leads to coding in the latent space, and the decoder part endeavors to convert the code into preliminary data (Figure 7). Autoencoders are a special type of feedforward neural networks where the input is the same as the output. They compress the input into a lower-dimensional code and then reconstruct the output from this representation. The code is a compact “summary” or “compression” of the input, also called the latent-space representation. Various methods have been proposed to block the data memorization by the network, including sparse AE (SpAE) and denoising AE (DAE) [21]. Trained properly, the coder part of an Autoencoder can be used to extract features; creating an unsupervised feature extractor.

4) *Recurrent Neural Networks (RNNs)*: In convolution networks, a kind of spatial dependencies in the data is addressed. But interdependencies between data are not confined to this model. For example in time-series, dependencies may be

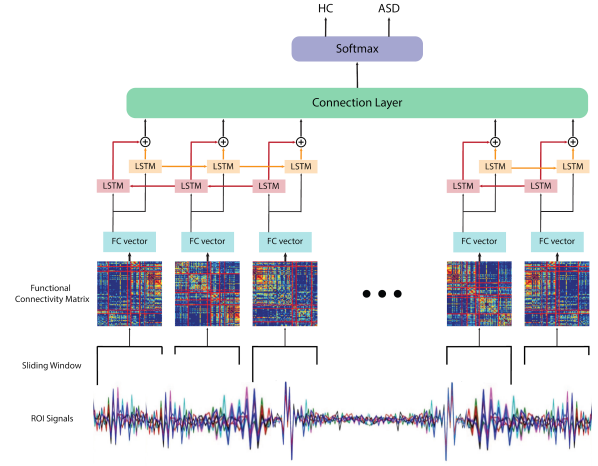


Fig. 8: Overall block diagram of an LSTM used for ASD detection.

highly distant from each other, on the other hand, the long-term and variable length of these sequences results in that the ordinary networks do not perform well enough to process these data. To overcome these problems, RNNs can be used. LSTM structures are proposed to extract long term and short term dependencies in the data (Figure 8). Another well-known structure called GRU is developed after LSTM, and since then, most efforts have been made to enhance these two structures and make them resistant to challenges (e.g., GRU-D [68] is used to find the lost data).

5) *CNN-RNN*: The initial idea in these networks is to utilize convolution layers to amend the performance of RNNs so that the advantages of both networks can be used; CNN-RNN, on the one hand, can find temporal dependencies with the aid of RNN, and on the other hand, it can discover spatial dependencies in data with the help of convolution layers [69]. These networks are highly beneficial for analyzing time series with more than one dimension (such as video) [70] but further to the simpler matter, these networks also yield the analysis of three-dimensional data so that instead of a more complex design of a 3D-CNN, a 2D-CNN with an RNN is occasionally used. The superiority of this model is due to the feasibility of employing pre-trained models. Figure 9 demonstrates the CNN-RNN model.

6) *CNN-AE*: In the construction of these networks, the principal aim and prerequisite have been to decrease the number of parameters. As shown before, changing merely the network layers to convolution markedly lessens the number of parameters; combining AE with convolution structures also makes significant contribution. This helps to exploit higher dimensional data and extracts more information from the data without changing the size of the database. Similar structures, with or without some modifications, are widely deployed for image segmentation [71], and likewise unsupervised network can be applied for network pre-training or feature extraction. Figure 10 depicts the CNN-AE network used for ASD detection. Tables I and II, provide the summary of papers published on detection and rehabilitation of ASD patients using DL,

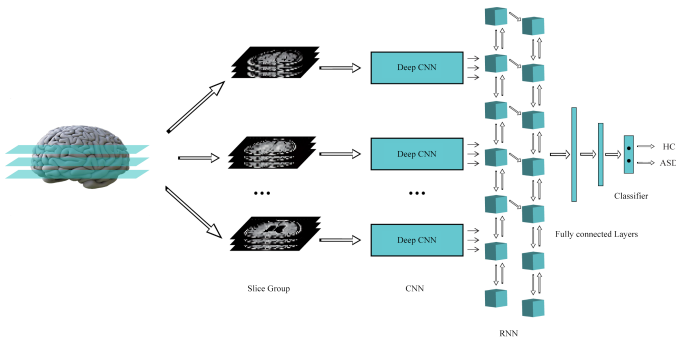


Fig. 9: Overall block diagram of a CNN-RNN used for ASD detection.

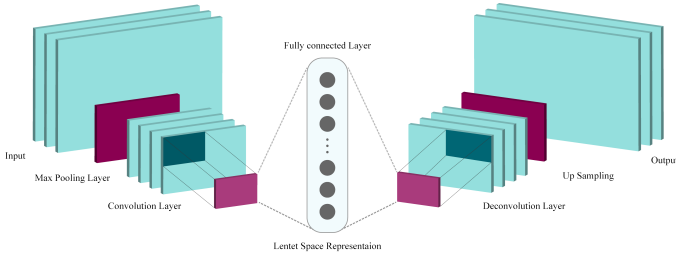


Fig. 10: Overall block diagram of a CNN-AE used for ASD detection.

respectively.

V. DEEP LEARNING TECHNIQUES FOR ASD REHABILITATION

Rehabilitation tools are employed in multiple fields of medicine and their main purpose is to help the patients to recover after the treatment. Various and multiple rehabilitation tools using DL algorithms have been presented. Rehabilitation tools are used to help ASD patients using mobile, computer applications, robotic devices, cloud systems, and eye tracking, which will be discussed below. Also, the summary of papers published on rehabilitation of ASD patients using DL algorithms are shown in Table II.

A. Mobile and Software Applications

Facial expressions are a key mode of non-verbal communication in children with ASD and play a pivotal role in social interactions. Use of BCI systems provides insight into the user's inner-emotional state. Valles et al. [72] conducted research focused on mobile software design to provide assistance to children with ASD. They aimed to design a smart iOS app based on facial images according to Figure 11. In this way, people's faces at different angles and brightness are first photographed, and are turned into various emoji so that the autistic child can express his/her feelings and emotions. In this group's investigation [72], Kaggle's (The Facial Expression Recognition 2013) and KDEF (Kaggle's FER2013 and Karolinska Directed Emotional Faces) databases were used to train the VGG-16. In addition, the LEAP system was adapted to train the model at the University of Texas. The research provided the highest rate accuracy of 86.44%. In

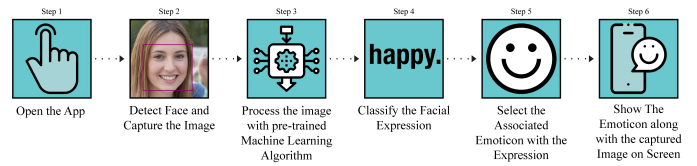


Fig. 11: Block diagram of ios application for ASD rehabilitation.



Fig. 12: Cloud system design for ASD rehabilitation.

another similar study, they achieved an accuracy of 78.32% [73].

B. Cloud Systems

Mohammadian et al. [74] proposed a new application of DL to facilitate automatic stereotypical motor movement (SMM) identification by applying multi-axis inertial measurement units (IMUs). They applied CNN to transform multi-sensor time series into feature space. An LSTM network was then combined with CNN to obtain the temporal patterns for SMM identification. Finally, they employed the classifier selection voting approach to combine an ensemble of the best base learners. After various experiments, the superiority of their proposed procedure over other base methods was proven. Figure 12 shows the real-time SMM detection system. First, IMUs, which are wearable sensors, are used for data collection; the data can then be analyzed locally or remotely (using Wi-Fi to transfer data to tablets, cell phones, medical center servers, etc.) to identify SMMs. If abnormal movements are detected, an alarm will be sent to a therapist or parents.

C. Eye Tracking

Wu et al. [75] proposed a model of DL saliency prediction for autistic children. They used DCN in their proposed paradigm, with a SM saliency map output. The fixation density map (FDM) was then processed by the single-side clipping (SSC) to optimize the proposed loss function as a true label along with the SM saliency map. Finally, they exploited an autism eye-tracking dataset to test the model. Their proposed model outperformed other base methods. Elbattah et al. [76] aimed to combine unsupervised clustering algorithms with deep learning to help ASD rehabilitation. The first step involved the visualization of the eye-tracking path, and the images captured from this step were fed to an autoencoder to learn the features. Using autoencoder features, clustering models are developed using the K-Means algorithm. Their method performed better than other state-of-art techniques.

TABLE I: Summary of articles published using DL methods for neuroimaging-based ASD detection.

Work	Datasets	Neuroimaging Modalities	Number of Cases	Pipelines	Image Atlas	Preprocessing Toolbox	High level Preprocessing	Inputs DNN	DNN Toolbox	DNN	Number of Layers	Classifier	K fold	Performance Criteria (%)
[24]	Clinical Acquisition	T-fMRI residual -fMRI	82 ASD 48 HC	NA	MNI152	FSL	SW	Single Mean Channel Input Single STD Channel Input Combined 2-Channel Input	NA	2CC3D	17	Majority Voting	NA	F1-Score = 89
[77]	Clinical Acquisition	T-fMRI	82 ASD 48 HC	NA	AAL	NA	SVE, C-SVE, H-SVE, Monte Carlo Approximation	Mean-Channel Sequence STD-Channel	NA	2CC3D	14	Sigmoid	NA	Acc = 97.32
[78]	HCP Dataset in the HAFNI Project	T-fMRI rs-fMRI	68 Subjects with 7 Tasks and 1 rs-fMRI Data	NA	NA	FSL	Dictionary Learning and Sparse Coding	Functional RNSs Maps	NA	3D-CNN	8	Softmax	NA	Acc = 94.61
[59]	Clinical Acquisition	T-fMRI	21 ASD 19 HC	NA	AAL	FSL	DA	ROIs Time-Series	Keras	LSTM	7	Sigmoid	10	Acc=69.8
[79]	Different Datasets	T-fMRI rs-fMRI Phenotypic Info	1711 ASD 15903 HC	NA	AAL	SPM SpeedyPP	Wavelet Transform and Different Techniques	FCM	Keras	2D-CNN	14	Softmax	NA	Ensemble AUROC=0.92 Ensemble Acc=85.19
[80]	Clinical Acquisition	T-fMRI	82 ASD 48 HC	NA	AAL	Neurosynth	SW Corrupting Strategy	Original fMRI Sequence Mean-Channel Sequence	NA	2CC3D	16	Sigmoid	NA	Acc= 87.1
[80]	ABIDE-I	rs-fMRI	41 ASD 54 HC	NA	AAL	FSL	Prediction Distribution Analysis	std-channel sequence Corrupt a ROI of Original Image	NA	2CC3D	16	Sigmoid	NA	Acc= 85.3
[81]	ABIDE-I ABIDE II	rs-fMRI	379 ASD, 395 HC 163 ASD, 230 HC	CPAC	All Atlases ABIDE CC-200	NA	FCM	Concatenating Voxel-Level Maps of Connectivity Fingerprints	NA	3D-CNN	7	Sigmoid	10	Acc= 73.3
[82]	ABIDE-I	rs-fMRI	505 ASD 530 HC	CPAC	AAL Dosenbach160	NA	FCM, DA	Masking Correlations	PyTorch	AE	NA	SLP	10	Acc=70.1 Sen=67.8 Spec=72.8
[83]	ABIDE-I	rs-fMRI	872 subjects	CPAC	HO	Nilearn	NA	Raw Images	NA	G-CNNs BrainNetCNN with Proposed Layers	5	Softmax	10	Acc=70.86 Acc= 68.7 Sen= 69.2 Spe= 68.3
[84]	ABIDE-I	rs-fMRI	474 ASD 539 HC	CCS	AAL	NA	FCM	Functional Connectomes	NA	NA	15	Softmax	5	Acc=70.86 Acc= 68.7 Sen= 69.2 Spe= 68.3
[85]	ABIDE-I	rs-fMRI	13 ASD 22 HC	NA	AAL	SPM8 REST DPARSF	Qcut, NMI Statistic Matrix	Pearson Correlation Coefficient Matrix NMI Matrix	NA	DAE	NA	NA	NA	Acc=54.49
[86]	ABIDE	rs-fMRI	11 ASD 16 HC	NA	NA	FSL BET	Convert NII Files to PNG Images	Preprocessed PNG Images	Caffe	LeNet-5	Standard	Softmax	NA	Acc=100 Sen=99.99 Spec=100
[87]	ABIDE-I	rs-fMRI	55 ASD 55 HC	NIAK	AAL	NA	FCM, Feature Selection	Whole-Brain FCPs	NA	Multiple SAEs	4	Softmax regression	5	Acc=86.36
[62]	ABIDE-I ABIDE-II ABIDE-I + II	rs-fMRI	54 ASD 62 HC 156 ASD 187 HC	NA	NA	SPM8	Dimension Reduction FFT	Images with 95 × 68, 79 × 68, and 79 × 95 Dimensions, Around the x, y, and z Axes	Keras with Theano backend	MCNNes	9	Binary SR	10	Acc=72.73 Sen=71.2 Spec=73.48
[88]	ABIDE	rs-fMRI	542 ASD 625 HC	CPAC	All Atlases	NA	Creating Stochastic Parcellations by Poisson Disk Sampling	Gray Matter Mask Parcellations	NA	3D-CNN	6	Various Methods	10	Acc=72
[89]	ABIDE-I	rs-fMRI	465 ASD 507 HC	DPARSF	AAL	NA	FCM	Edge Weights of Subjects' Brain Graph	Keras	VAE	3	NA	NA	NA
[90]	ABIDE-I	rs-fMRI	539 ASD 573 HC	CCS	Craddock 200	Neurosynth	DA	Mean Time Courses from ROIs	Keras	LSTM	5	Sigmoid	10	Acc=68.5
[91]	ABIDE	rs-fMRI, Phenotypic Info	505 ASD 530 HC	NA	CC200	DPABI	Slicetiming, Spatial Standardization, Smoothing, Filtering, Removing Covariates, FCM, AE-MKFC	4005-Dimensional Eigenvector	NA	SAE	3	Clustering	NA	Acc=61 F1-Score=60.2
[92]	ABIDE	rs-fMRI	42 ASD 42 HC	NA	NA	FSL	Independent Components (Time Course, Power Spectrum and Spatial Map)	Time Courses of Each Subject	NA	SAE	9	Softmax	21	Acc=87.21 Sen=89.49 Spec=83.73
[93]	ABIDE-I	rs-fMRI	NY site UM site US site UC site	CCS	AAL	Neurosynth	DA	fMRI ROI Time-Series, Functional Connectivity	Keras	LSTM	6	Sigmoid	10	Acc=74.8
[94]	ABIDE-I	rs-fMRI	408 ASD 401 HC	CPAC	HO AAL CC200	FSL	NA	3 Different FCM+ Demographic Data	Keras	DANN	25	Sigmoid	10	Acc=73.2 Sen=74.5 Spec=71.7
[95]	ABIDE	rs-fMRI	At Least 60 Subjects	CCS	AAL	FSL	DTL-NN Framework: Offline Learning, Transfer Learning FCM	FC Patterns	NA	SSAE	4	Softmax regression	5	Avg Acc= 67.1 Avg Sen=65.7 Avg spec=68.3 AUC=0.71
[96]	ABIDE I+II	rs-fMRI	993 ASD 1092 HC	NA	AAL Schaefer-100 HO Schaefer-400	FAST BET FAST	NA	Mean Time-Series within Each ROI	NA	1D-CNN	5	Softmax	10	Acc=68

[97]	ABIDE-I	rs-fMRI	529 ASD 573 HC	All Pipelines	NA	NA	Single Volume Image Generator	Glass Brain and Stat Map Images	Keras	4 Deep Ensemble Classifier techniques	16	Sigmoid	NA	Acc=87 F1-score=86 Recall=85.2 Pre=86.8
[98]	ABIDE-II	rs-fMRI	303 ASD, 390 HC	NA	NA	FSL	NA	1D Time Series from Voxels	NA	ID-CAE	14	NA	NA	Acc= 63.3
[99]	ABIDE	rs-fMRI	40 ASD, 40 HC	CCS	NA	NA	Thresholding Based Segmentation	WM, GM, CSF	NA	AlexNet	Standard	Softmax	NA	Acc=82.61
[100]	ABIDE	rs-fMRI	Whole Dataset	All Pipelines	Parcellated into 200 Regions	NA	DA Using SMOTE and Graph Network Motifs, FCM	Upper Triangle Part of the Correlation Matrix	NA	ASD-DiagNet	Proposed	SLP	NA	Acc=82 Sen=79.1 Spec=83.3
[60]	ABIDE-I	rs-fMRI	12 ASD 14 HC	CPAC	SCSC	NA	Time Series Extraction from Different Regions, Connectivity Matrix, SMOTE Algorithm	FCM	PyTorch	Auto-ASD-Network	Proposed	SVM	5	Acc=80 Sen=73 Spec=83
[61]	ABIDE-I	rs-fMRI	505 ASD 530 HC	CPAC	CC400	NA	FCM	FCM	NA	2D-CNN	20	MLP	10	Acc=70.20 Sen=77.00 Spec=61.00
[101]	ABIDE	rs-fMRI	505 ASD 530 HC	NA	NA	NA	FCM	1D-Vector of FCM	NA	1D CNN -AE	7	Softmax	NA	Acc=70 Sen=74 Spec=63
[102]	ABIDE-I	rs-fMRI	539 ASD 573 HC	NA	NA	FreeSurfer	NA	Single 3D Image	Theano	3D-FCNN	13	Softmax	6	Mean DSC=91.56 Mean MHD=14.05
[103]	ABIDE-I	rs-fMRI	501 ASD 553 HC	DPARSF	AAL	NA	FCM, Converting to 1D-Vector	1000 Features Selected by the SVM-RFE	NA	SSAE	3	Softmax	Different Folds	Acc=93.59 Sen=92.52 Spec=94.56
[104]	ABIDE-I	rs-fMRI	100 ASD 100 HC	NA	NA	FSL FEAT	Online Dictionary Learning and Sparse Representation Techniques, Generating Spatial Overlap Patterns	4D Matrix with 150 3D Network Overlap Maps	Theano	3D-CNN	14	NA	10	Average Acc= 70.5 Average Sen= 74 Average Spec= 67
[105]	ABIDE-I	rs-fMRI & Phenotypic Info	529 ASD 571 HC	CPAC	HO	FSL	Population Graph Construction, Feature Selection Strategies (RFE, PCA, MLP, AE)	Population Graph	Scikit-learn	GCN	11	Softmax	10	Acc=80.0
[106]	ABIDE-I	rs-fMRI & Phenotypic Info	403 ASD 468 HC	CCS	CC200	NA	DA	Mean Time-Series from ROIs	Keras	LSTM	6	Sigmoid	10	Acc=70.1
[107]	ABIDE-I	rs-fMRI & S-MRI & Phenotypic Info	505 ASD 530 HC	CPAC	Craddock 200	NA	FCM	1D-Vector of FCM	NA	Two SdAE + MLP	NA	Softmax	10	Acc=70 Sen=74 Spec=63
[108]	Clinical Acquisition	rs-fMRI Fetal BOLD fMRI	75 Qualified Subjects	NA	NA	FSL Brainsuite SPM8 CONN	Extraction of Fetal Brain fMRI Data, SW	Mean Time Series of 3D fMRI Volumes	PyTorch	3D-CNN	7	Sigmoid	NA	F1-score=84 AUC=91
[109]	ABIDE-I	rs-fMRI	116 ASD 69 HC	NA	AAL	SPM8	Segmentation, Average Mean Time Series of Each ROI	Rs-fMRI + GM+WM Data Fusions	Theano	DBN	6	LR	10	Acc=65.56 Sen=84 Spec=32.96
[110]	IMPAC	rs-fMRI s-MRI	418 ASD 497 HC	NA	All atlases	NA	FCM, Features Extraction from S-MRI	FCM Vector Anatomical Features Combination of Both Anatomical and Connectivity FCM Vector	Keras Tensor-Flow Caffe	Different Networks	8	Various Methods	3	AUC= 80
[111]	ABIDE-I	rs-fMRI s-MRI	368 ASD 449 HC	CPAC	AAL CC200 Destrieux	FreeSurfer	FCM, Fisher Score	1D-Vector of FCM	NA	Ensemble of 5 Stacked AEs and MLP	31	Label Fusion Using the Average of Softmax Probabilities	10	Acc= 85.06 Sen= 81 Spec= 89
[112]	NDAR	rs-fMRI s-MRI	61 ASD 215 HC	NA	NA	NA	Data-Driven Landmark Discovery Algorithm, Patch Extraction	50 Patches Extracted from 50 Landmarks	NA	Multi-Channel CNN	13	Softmax	10	Acc=76.24
[63]	NDAR	All Modalities	78 ASD 124 HC	NA	Proposed Atlas	FSL BET	PICA, Extraction of PSD	PSDs of 34 Components	NA	34 SAEs	Each SAE Has 2 Layers	PSVM	NA	Acc=88.5 Sen=85.1 Spec=90.4
[113]	NDAR	s-MRI	60 ASD, 211 HC	NA	NA	In-House Tools	3D Patches Extraction	Patch Size 16x64x16	NA	DDUNET	11 Blocks	NA	5	NA
[114]	ABIDE-I NDAR/Pitt NDAR/IBIS	s-MRI	21 ASD, 21 HC 16 ASD, 16 HC 10 ASD, 10 HC	NA	NA	FSL iBEAT	Segmentation, Shape Feature Extraction	CDF Values of Features	NA	SNCAE	NA	Softmax	NA	Acc=96.88

[115]	ABIDE-I	s-MRI	78 ASD 104 HC	NA	Destrieux	FreeSurfer	Construction of Individual Network, F-score	3000 Top Features	NA	SAE	3	Softmax	10	Acc=90.39 Sen=84.37 Spec=95.88
[116]	HCP	s-MRI	1113 HC	NA	Desikan-Killia	FreeSurfer	Normalization. Apply One-Hot Coding	Preprocessed Images	Tensor-Flow	DEA	3	NA	10	AUC=63.9
	ABIDE-I		83 ASD 105 HC						Keras					
[117]	ABIDE	s-MRI	1112 Subjects	NA	NA	SPM12	NA	32 Slices Along Each Axial, Coronal, and Sagittal	Keras	DCNN	17	Sigmoid	NA	Acc=84 Sen=77 Spec=85
	CombiRx													
[118]	ABIDE-II	s-MRI	NA	NA	DKT	FreeSurfer	Segmentation	Coronal, Axial and Sagittal 2D Slices	PyTorch	FastSurfer CNN	Proposed	Softmax	NA	NA
[119]	ABIDE-I	s-MRI	500 ASD 500 HC	NA	HO Cortical and Subcortical Structural Atlas	FSL	GABM Method, New Chromosome Encoding Scheme	Preprocessed MRI Scans	NA	3D-CNN	11	Softmax	5	Acc=70
[120]	Clinical Acquisition	s-MRI	48 HC	NA	NA	FreeSurfer	Sparse Annotations, DA	Image Patch	Caffe	3D-CNN	18	Softmax	NA	Acc=91.6 AUC=94.1
[121]	ABIDE-I	rs-fMRI	270 ASD 305 HC	CPAC	Brain-Netome Atlas (BNA)	NA	Filtering, Calculating Mean Time Series for ROIs Using BrainNetome Atlas (BNA), Normalization	Mean Time Series Data Stacked Across ROIs	NA	CNN-GRU	14	Sigmoid	5	Acc=74.54 Sen=63.46 Spec=84.33
[122]	Clinical Acquisition	fNIRS	25 ASD 22 HC	No	No	No	Transformation of the Time Series to Three Variants	PM, GM, SM	Keras	1D CNN-LSTM	NA	Bagging	NA	Acc=95.7 Sen=97.1 Spec=94.3
[123]	Clinical Acquisition	fNIRS	25 ASD 22 HC	No	No	No	SW Converted into the 3D Tensor	3D Tensor	NA	CGRNN	7	NA	NA	Acc=92.2 Sen=85.0 Spec=99.4
[124]	Different Datasets	s-MRI	NA	NA	Various Methods	FreeSurfer FSL SPM12 VolBrain	Geometric DA	3D Cortical Mask	Theano	ConvNet	U-Nets	NA	8	NA
[125]	ABIDE I+II	rs-fMRI	620 ASD 2085 HC	CPAC	HO	FSL	Performed an Automatic Quality Control, Visually Inspection, 9 Temporal Summary Measures, Mean and STD of the Summary Measures, Normalization, Occlusion of Brain Regions	Each Summary Measure	NA	MM-ensemble (3D-CNN)	7	Majority Voting	5	Acc=64 F1-Score=66
[126]	ABIDE-I	rs-fMRI Phenotypic Information	184 ASD 110 HC	CPAC	NA	NA	Down Sampling	Raw 4D Volume	NA	3D-CNN C-LSTM	21	Softmax	5	Acc=77 F1-score=78
[127]	ABIDE-I	rs-fMRI and s-MRI	403 ASD 468 HC	NA	264 ROIs Based Parcellation Scheme	AFNI FSL MATLAB	FCM, Feature Extraction (Different Features)	Normalized Features	NA	AE	7	DNN	10	Acc= 79.2 AUC= 82.4
[128]	ABIDE-I	rs-fMRI	505 ASD 530 HC	CPAC	CC200	NA	FCM	1D-Vector of FCM	PyTorch	CapsNet	Standard	K-Means Clustering	10	Acc=71 Sen=73 Spec=66

TABLE II: Summary of papers published on rehabilitation of ASD patients using DL algorithms.

Work	Datasets	Type of Applications	Number of Cases	Preprocessing	Inputs DNN	DNN Toolbox	DNNs	Number of Layers	Classifier	K fold	Performance Criteria (%)
[129]	OSIE	—	20 ASD 19 HC	HFM Construction, Filtering Normalizing, DA	HFM, Natural Scene Images	Caffe TensorFlow	VGGNet	50	Softmax	13	Acc=85 Sen=80 Spec=89
[73]	KDEF	Facial Expression Recognition	70 Individuals	DA	RGB Images (562x762)	Keras	DCNN	44	Softmax	NA	Acc=78.32
[130]	Clinical Acquisition	Detecting Audio Regimes That Directly Estimate ASD Severity Social Affect scores	33 ASD	MFCC Spectrograms	32 Spectrograms	NA	Noisemes Network DiarTK Diarization Network	Standard Network	Synthetic RF	NA	Acc=84.7
[72]	Kaggle's FER2013 KDEF	Facial Expression Recognition	NA	No	48x48-Pixel Images	Keras (TensorFlow Backend)	DCNN	44	Softmax	NA	Acc=86.44
[131]	SALICON	ASD Classification	14 ASD 14 HC	SalGAN Model, Feature Extraction	Sequence of Image Patches	NA	SP-ASDNet	11	NA	NA	Acc=57.90 Rec=59.21 Pre=56.26
[132]	BigFaceX	Facial Expression Recognition	196 Subjects	SW, Merge in the Channel Dimension, DA	5-channel Sub-Sequence Stacks within a Specific Time Window	Keras	TimeConvNet	PreTrain Nets	Softmax	NA	Acc=97.9
[133]	Different Datasets	Suitable Courseware for Children with ASD	NA	Interactive and Intelligent Chatbot , NLP, Visual Aid	Different Inputs	NA	Different Nets	NA	NA	NA	NA
[134]	Camera Images	Estimating Visual Attention in Robot-Assisted Therapy	6 ASD and ID	Resizing, Frame Extraction, Visual Inspection Face Detection (Viola-Jones), Feature Extraction (HOG Descriptors)	5 Facial Landmarks - 36 HOG Descriptors	NA	R-CNN MTCNN	VGG-16 Cascaded CNNs Architecture	K-NN Naive	10	Acc= 88.2 Pre=83.3 Sen=83.0 Spec=87.3
[135]	Sensor Data	Automatic SMM detection	6 ASD 5 HC	Resampling, Filtering, SW	Time-Series of Multiple Sensors	Keras	CNN-LSTM	13	Majority Voting	NA	NA
[136]	KOMAA	Facial Expression Recognition	55 subjects	Segmentation, Different Features, Z-scores	Greedy Forward Feature Selection	NA	CNN	9	SVM	NA	Acc=96
[137]	Story-Telling Narrative Corpora	ASD Classification	31 ASD 36 HC	DA, ChineseWord2Vec	32-Dimensional Word Vector	NA	LSTM	1	Coherence Representation of LSTM Forget Gate	NA	Acc=92
[138]	Ext-Dataset (video dataset)	ASD Classification using Eye Tracking	136 ASD 136 HC	TLD Method, Accumulative Histogram Computation	Angle Histogram, Length Histogram and Fused Histogram,	Keras	LSTM	4	NA	10	Acc=92.6 Sen=91.9 Spec=93.4 SIM=67.8 CC=76.9 AUC-J=83.4
[139]	MIT1003	Predicting Visual Attention of Children with ASD.	300 Images	NA	Raw Images	NA	DCN	26	NA	NA	Acc=55.13 Avg Recall=75 Avg Acc=71
[75]	Scan Path Data, Including Location and Duration	ASD Classification	14 ASD 14 HC	DA Methods	Image, Data Points	Pytorch	ResNet18	Standard	Softmax	NA	Acc=99.53 Sens=99.39 Spec=100
[140]	UCI Machine Learning Repository	ASD Classification	704	Different Methods	Preprocessed Data	NA	CNN	7	NA	NA	Acc=99.53 Sens=99.39 Spec=100
[76]	Eye Tracking Scanpath	ASD Classification	29 ASD 30 HC	Visualization of Eye-Tracking Scanpaths Scaling Down, PCA	100*100 Image	Keras, Scikit-Learn	AE	8	K-Means Clustering	NA	Silhouette score=60
[141]	Video Data	Engagement Estimation of Children with ASD During a Robot-Assisted Autism Therapy	30 children	NA	Cropped Face Images (256 *256)	Keras with TensorFlow Backend	CultureNet	R-CNN + ResNet50+ 5FC layers	Softmax	NA	ICC=43.35 CCC=43.18 PC=45.17
[142]	YouTube ASD Dataset	Modeling Typical and Atypical Behaviors in ASD Children	68 video Clips	Different Methods	Sequences of Individual Frames at a Rate of 30 fps	openCV, Caffe	DCNN	NA	DT	5	Avg Pre=73 Avg Recall=75 Avg Acc=71
[143]	Video Dataset	Behavioral Data Extracted from Video Analysis of Child-Robot Interactions.	5 ASD 7 HC	Segmentation, Upper Body tracking, Laban Movement Analysis to Drive Weight, Different features	3 Movement Features with 68 Facial Key-Points	NA	CNN	10	Softmax	NA	Acc=88.46 Pre=89.12 Recall=88.53
[144]	Video Dataset	Developing Automatic SMM Detection Systems	6 ASD	Resampling, Filtering, SW, Data Balancing, Normalizing	Time-Series of Multiple Accelerometer Sensors	DeepPy Library	CNN	8	SVM	NA	F1-score=95
[145]	ASD Screening	Autism Screening	513 ASD 189 HC	Cleaning Missing Values and Outliers, Visualization, Identity Mapping	The Embedded Categorical Variables are Concatenated with Numerical Features as New Feature Vectors	NA	DENN	4	Sigmoid	NA	Acc=100 Spec=99 Sen=100 F1-score=99
[146]	ASD Screening Datasets	Classification of Adults with ASD	—	Handling of Missing Values, Variable Reduction, Normalization, and Label Encoding	Normalized Variables	Keras	DNN	7	Sigmoid	NA	Acc=99.40 Sen=97.89 Spec=100

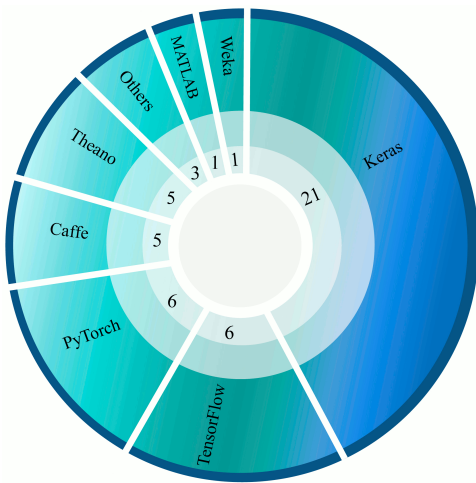


Fig. 13: Number of DL tools used for the diagnosis and rehabilitation of ASD patients in reviewed papers.

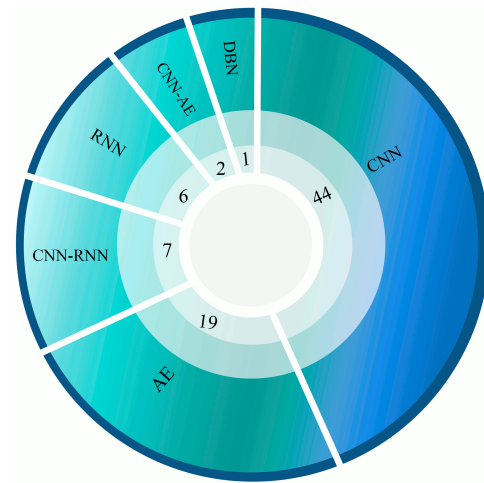


Fig. 14: Number of DL networks used for ASD detection and rehabilitation in the reviewed works.

VI. DISCUSSION

In this study, we performed a comprehensive overview of the investigations conducted in the scope of ASD diagnostic CAD systems as well as DL-based rehabilitation tools for ASD patients. In the field of ASD diagnosis, numerous papers have been published using functional and structural neuroimaging data as well as rehabilitation tools, as summarized in Table III in the appendix. A variety of DL toolboxes have been proposed for implementing deep networks. In Tables I and II the types of DL toolboxes utilized for each study are depicted, and the total number of their usage is demonstrated in Figure 13. The Keras toolbox is used in the majority of the studies due to its simplicity. Keras offers a consistent high-level application programming interface (APIs) to build the models more straightforward, and by using powerful backends such as TensorFlow, its performance is sound. Additionally, due to all pre-trained models and available codes on platforms such as GitHub, Keras is quite popular among researchers.

Number of DL networks used for the ASD detection in the reviewed works is shown in Figure 14. Among the various DL architectures, CNN is found to be the most popular one as it has achieved more promising results compared to other deep methodologies. The autoencoder, as well as RNN, have yielded favorable results. It can be noted that in recent years, the number of DL-based papers has increased exponentially due to their sound performance and also the availability of vast and thorough datasets.

The number of various classification algorithms used in DL networks are shown in Figure 15. One of the best and most widely used is the Softmax algorithm (Tables I and II). It is most popular since it is differentiable in the entire domain and computationally less expensive.

VII. CHALLENGES

Some of the most substantial challenges in ASD diagnosis scope using DL-based techniques are addressed in this section, which comprise database and algorithmic problems. There are only two-class brain structural and functional datasets (ASD



Fig. 15: Number of various classification algorithms used for the detection of ASD and rehabilitation in DL.

and healthy) available in the public domain. Hence, researchers are not able to broaden their investigation to all sub-types of ASD. Two of the cheapest and most pragmatic functional neuro-screening modalities for diagnosis of ASD are EEG, and fNIRS. But unfortunately the deficiency of freely available datasets has resulted in little research in this area. Another obstacle is that multi-modality databases such as EEG-fMRI are not available to researchers to evaluate the effectiveness of incorporating information of different imaging modalities to detect ASD. Although fMRI and sMRI data are ubiquitous in the ABIDE dataset, the results of merging these structural and functional data for ASD diagnosis using DL have not yet been investigated. Another problem grappling the researchers is designing the DL-based rehabilitation systems with hardware resources. Nowadays, assistive tools such as Google Colab are available to researchers to improve the processing power; however, the problems still prevail when implementing these systems in real-world scenarios.

VIII. CONCLUSION AND FUTURE WORKS

ASD is typically characterized by social disorders, communication deficits, and stereotypical behaviors. Numerous computer-aided diagnosis systems and rehabilitation tools have been developed to assist patients with autism disorders. In this survey, research on ASD diagnosis applying DL and functional and structural neuroimaging data were first assessed. The researchers have taken advantage of deep CNNs, RNNs, AEs, and CNN-RNN networks to improve the performance of their systems. Boosting the accuracy of the system, the capability of generalizing and adapting to differing data and real-world challenges, as well as reducing the hardware power requirements to the extent that the final system can be utilized by all are the principal challenges of these systems. To enhance the accuracy and performance of CADS for ASD detection in the future, deep reinforcement networks (RL) or GANs can be exploited. Scarcity of data is always an paramount problem in the medical field that can be resolved relatively with the help of these deep GANs. Also, as another direction for future works, handcrafted features can be extracted from data and fed to DL networks in addition to raw data; this can help increasing performance by adding the potential of traditional methods to DL-based models.

Many researchers have proposed various DL-based rehabilitation tools to aid the ASD patients. Designing a reliable, accurate, and wearable low power consumption DL algorithm based device is the future tool for ASD patients. An achievable rehabilitation tool is to wear smart glasses to help the children with ASD. These glasses with the built-in cameras will acquire the images from the different directions of environment. Then the DL algorithm processes these images and produces meaningful images for the ASD children to better communicate with their surroundings.

APPENDIX A STATISTICAL METRICS

This section demonstrates the equations for the calculation of each evaluation metric. In these equations, True positive (TP) is the correct classification of the positive class, True negative (TN) is the correct classification of the negative class, False positive (FP) is the incorrect prediction of the positives, False negative (FN) is the incorrect prediction of the negatives.

$$Accuracy(Acc) = \frac{TP + TN}{TP + TN + FP + FN} \quad (1)$$

$$Specificity(Spec) = \frac{TN}{TN + FP} \quad (2)$$

$$Sensitivity(Sen) = \frac{TP}{TP + FN} \quad (3)$$

$$Precision(Prec) = \frac{TP}{TP + FP} \quad (4)$$

$$F1 - Score = 2 * \frac{Prec * Sens}{Prec + Sens} \quad (5)$$

RECEIVER OPERATING CHARACTERISTIC CURVE (ROC-CURVE)

The receiver operating characteristic curve (ROC-curve) depicts the performance of the proposed model at all classification thresholds. It is the graph of true positive rate vs. false positive rate (TPR vs. FPR). Equations for calculation of TPR and FPR are presented below.

$$TPR = \frac{TP}{TP + FN} \quad (6)$$

$$FPR = \frac{FP}{FP + TN} \quad (7)$$

AREA UNDER THE ROC CURVE (AUC)

AUC presents the area under the ROC-curve from (0, 0) to (1, 1). It provides the aggregate measure of all possible classification thresholds. AUC has a range from 0 to 1. A 100% wrong classification will have AUC value of 0.0, while a 100% correct classified version will have the AUC value of 1.0. It has two folded advantages. One is that it is scale-invariant, which implies how well the model is predicted rather than checking the absolute values. The second advantage is that it is classification threshold-invariant as it will verify the performance of the model irrespective of the threshold being selected.

APPENDIX B

Table III shows details of Deep Nets in all the papers reviewed in this study.

ACKNOWLEDGMENT

MB is supported by a NHMRC Senior Principal Research Fellowship (1059660 and 1156072). MB has received Grant/Research Support from the NIH, Cooperative Research Centre, Simons Autism Foundation, Cancer Council of Victoria, Stanley Medical Research Foundation, Medical Benefits Fund, National Health and Medical Research Council, Medical Research Futures Fund, Beyond Blue, Rotary Health, A2 milk company, Meat and Livestock Board, Woolworths, Avant and the Harry Windsor Foundation, has been a speaker for Astra Zeneca, Lundbeck, Merck, Pfizer, and served as a consultant to Allergan, Astra Zeneca, Bioadvantex, Bionomics, Collaborative Medicinal Development, Lundbeck Merck, Pfizer and Servier - all unrelated to this work.

TABLE III: Details of Deep Nets. For ASD diagnosis and Rehabilitation.

Work	Network	Details for Deep Networks	Dropout	Classifier	Optimizer	Loss Function
[24]	2CC3D	CNN Layers (6) + Pooling Layers (4) + FC Layers (2)	2 (rate=0.5) 2 (rate=0.65)	Sigmoid	NA	BCE
[77]	2CC3D	CNN Layers (6) + Pooling Layers (4) + FC Layers (3)	NA	Sigmoid	NA	NA
[78]	3D-CNN	CNN Layers (2) + LReLU Activation + Pooling Layers (1) + FC Layers (1)	3 (rate=NA)	Softmax	SGD	MNLL
[59]	LSTM	LSTM Layers (1) + Pooling Layers (1) + FC Layers (3)	1 (rate=0.5)	Sigmoid	Adadelta	MSE
[79]	CNN	CNN Layers (2) + ReLU Activation + BN Layers (4) + FC Layers (3)	2 (rate=0.3) 2 (rate=0.7)	Softmax	Adam	NA
[80]	2CC3D	CNN Layers (6) + Pooling Layers (4) + FC Layers (2)	2 (rate=NA)	Sigmoid	NA	NA
[81]	CNN	CNN Layers (2) + ELU Activation + Pooling Layers (2) + FC Layers (2)	NA	Sigmoid	SGD	NA
[82]	AE	Standard AE with Tanh Activation	NA	SLP	NA	MSE BCE
[83]	G-CNN	Proposed G-CNN with 3 Layer CNN	(rate=0.3)	Softmax	Adam	NA
[84]	BrainNetCNN with Proposed Layers	Element-wise layer (1) + E2E layers (2) + E2N layer (1) + N2G layer (1) + FC layers (3)+ Leaky ReLU Activation+ Tanh Activation	5 (rate=0.5) 1 (rate= 0.6)	Softmax	Adam	Proposed Loss Function
[85]	DAE	Standard DAE	NA	NA	NA	Proposed Loss function
[86]	LeNet-5	Standard LeNet-5 Architecture	NA	Softmax	NA	NA
[87]	SAE	SAE with LSF Activation	NA	Softmax	L-BFGS	NA
[62]	MCNNes	CNN Layers (3) + ReLU Activation + Pooling Layers (3) + FC Layers (1)	1 (rate=0.5)	Binary SR	Adam Adamax	BCE
[88]	3D-CNN	CNN Layers (2) + ELU Activation + Pooling Layers (2) + FC Layers (3)	NA	Sigmoid	SGD Adam	BCE MSD
[89]	VAE	VAE with 3 Layers	NA	NA	Adadelta	Proposed Loss Function
[90]	LSTM	LSTM Layers (1) + Pooling Layers (1) + FC Layers (1)	1(rate=0.5)	Sigmoid	Adadelta	BCE
[91]	SAE	SAE Layers (3) + Sigmoid Activation	NA	Clustering	Proposed Opt.	NA
[92]	SAE	SAE Layers (8) + Sigmoid Activation	NA	SR	L-BFGS	MSE BCE
[93]	LSTM	LSTM Layers (2) + Pooling Layers (1) + FC Layers (2)	NA	Sigmoid	Adam	MSE
[94]	Multichannel DANN	3 MLP (1 Dropout Layer and 4 Dense Layers) + Self-Attention (3) + Fusion (3) + Aggregation Layer + Dense Layer (1) + ReLU, ELU, Tanh Activations	1 (rate=NA)	Sigmoid	NA	CE
[95]	SSAE	3 SSAE Layers	NA	Softmax	Scaled Conjugate Gradient Descent	Proposed Loss Function
[96]	1D-CNN	CNN Layers (1) + Pooling Layers (1) + FC Layers (1)	(rate=0.2)	Softmax	Adam	NA
[97]	CNN	CNN Layers (6) + Pooling Layers (4) + BN Layers (2) + FC Layers (2)	1 (rate=0.25)	Sigmoid	Adam	Propose Loss Function
[98]	1D CAE-CNN	Encoder (4 layers) + Decoder (4 layers) + CNN layers (2) + pooling layers (2) + FC layers (2)	NA	NA	NA	NA
[99]	AlexNet	Standard AlexNet Architecture	NA	Softmax	NA	CE
[100]	ASD-DiagNet	Proposed DiagNet	NA	SLP	NA	NA
[60]	Auto-ASD-Network	Proposed Auto-ASD-Network	NA	SVM	NA	NLLF
[61]	CNN	CNN layers (7) + Pooling layers (7) + FC layers (3)	1 (rate=0.25)	MLP	NA	NA
[101]	2 SdAE-CNN	Proposed SDAE-CNN with 7 Layers CNN	NA	Softmax	NA	NA
[102]	3D-FCNN	CNN Layers (9) + PReLU Activation + FC Layers (3)	NA	Softmax	SGD	CE
[103]	SSAE	2 Layers SSAE	NA	Softmax	NA	NA
[104]	3D-CNN	CNN layers (7) + Pooling Layers (3) + FC Layers (2) + Log-Likelihood Activation	2 (rate=0.2)	NA	SGD	MNLL
[105]	GCN AE	GCN with ReLU and Sigmoid Activation SAE with Tanh Activation	(rate=0.3)	Softmax	NA	CE MSE
[106]	LSTM	Proposed Deep Network	(rate=0.5)	Sigmoid	Adadelta	BCE MSE
[107]	2 SdAE-MLP	Proposed 2-SDAE-MLP Network	NA	Softmax	NA	MSE
[108]	3D-CNN	CNN Layers (2) + ReLU Activation + Pooling Layers (2) + FC Layers (2)	NA	Sigmoid	SGD	BCE
[109]	DBN	DBN with 5 Hidden Layers	NA	LR	NA	NA
[110]	FeedFWD	Dense layers (5) + LReLU activation	3 (rate= NA)	NA	Adam	BCE
[111]	Ensemble of 5 SAEs and MLPs	5 [AE (3) + MLP (2)] + Softmax	5 (rate=NA)	Averaging the Softmax Activation Probabilities	NA	NA
[112]	Multi-Channel CNN	CNN Layers (5) + ReLU Activation + Pooling Layers (2) + FC Layers (5)	NA	Softmax	NA	CE
[63]	34 SAEs	34 [SAE network (2)]	NA	PSVM	L-BFGS	NA
[113]	DDUNET	Proposed DDUNET with 11 blocks and ReLU Activation	(rate=0.1)	NA	SGD	CE
[114]	SNAE	Proposed SNAE Network	NA	Softmax	NA	NA
[115]	SpAE	SpAE with 2 Networks	NA	Softmax	NA	MSE
[116]	DAE	AE (3) + SELU Activation	NA	NA	Adam	Sum of MSE + 2 CE + CC
[117]	DCNN	CNN Layers (6) + ReLU Activation + Pooling Layers (6) + FC Layers (4)	NA	Sigmoid	Adam	BCE
[118]	FastSurfer CNN	Proposed FastSurfer CNN Network	NA	Softmax	Adam	Logistic & Dice Losses
[119]	3D-CNN	CNN Layers (3) + ReLU Activation + Pooling Layers (3) + FC Layers (2)	2 (rate=0.5)	Softmax	Adadelta	CE
[120]	3D-UNET	DCNN Layers (7) + ReLU Activation + Pooling Layers (2) + BN Layers (6)	2 (rate=0.5)	Softmax	SGD	weighted CE
[121]	CNN-GRU	CNN Layers (4) + GRU Layers (2) + ReLU Activation + Pooling Layers (2) + FC Layers (5)	NA	Sigmoid	Adam	BCE
[122]	1D CNN - LSTM	Proposed 1D-CNN LSTM with ReLU Activation	(rate=0.2)	Softmax	Adam	CCE
[123]	CGRNN	CNN layers (3) + ReLU Activation + Pooling Layers (1) + GRU Layers (1) + Sigmoid Activation + FC Layer (1)	1 (rate=0.5)	NA	Adam	BCE
[124]	ConvNet	Variation of the U-net Convolutional Architecture	NA	NA	Adam	Proposed Loss Function
[125]	3D-CNN	CNN Layers (2) + ELU Activations + Pooling Layers (2) + FC Layers (2)	NA	Sigmoid	SGD	BCE
[126]	3DCNN C-LSTM	CNN Layers (8) + Conv-Bi LSTM Layers (2) + Sigmoid Activation (for LSTM) + Pooling Layers (1) + FC Layers (1)	8 (rate=0.2)	Softmax	Adam	CE
[127]	AE	Proposed AE with 7 Layers	NA	DNN	NA	NA
[128]	CapsNets	Standard Architecture	NA	K-Means Clustering	Adam	Proposed Loss Function
[129]	VGGNets + ASDNet	CNN Layers (27) + ReLU Activation + Pooling Layers (10) + FC Layers (6)	6 (rate=0.5)	Softmax	SGD	CE
[73]	DCNN	CNN Layers (7) + Activation+ Pooling Layers (13) + FC Layers (3) + BN Layers (10)	7 (rate=0.25) 3 (rate=0.5)	Softmax	SGD	NA
[130]	Noisemes net DiarFK Diarization net	Standard Networks	NA	RF	NA	NA
[72]	DCNN	CNN Layers (7) + ELU Activation + Pooling Layers (13) + FC Layers (3) + BN Layers (10)	7 (rate=0.25) 3 (rate=0.5)	Softmax	SGD	NA
[131]	SP-ASDNet	CNN Layers (2) + LSTM Layers (2) + Pooling Layers (3) + FC Layers (2)	2 (rate=NA)	NA	Adam	BCE
[132]	TimeConvNet	Convolutional Spatiotemporal Encoding Layers+ Backbone Convolutional Neural Network Architecture (Mini-Xception, ResNet20, MobileNetV2)	NA	Softmax	Adam	CCE
[133]	Different Networks	Proposed Structure	NA	NA	NA	NA
[134]	RCNN MTCNN	VGG-16 Cascaded CNNs Architecture	NA	KNN	NA	NA
[135]	CNN-LSTM	CNN Layers (3) + LSTM Layers (1) + ReLU Activation + Pooling Layers (3) + FC Layers (3)	1 (rate=0.5) 1 (rate=0.2)	Softmax	SGD	NA
[136]	CNN	CNN Layers (4) + Pooling Layers (2) + FC Layers (2)	NA	Softmax	NA	NA
[137]	LSTM	LSTM layer (1)	NA	Coherence Representation	NA	NA
[138]	LSTM	LSTM Layers (3) + Sigmoid Activation + FC Layers (1)	NA	NA	NA	CE
[139]	DCN	CNN Layers (17) + Pooling Layers (3) + Deconvolution Layers (3) + Learned Priors (3)	NA	NA	NA	Proposed Loss Function
[75]	Pretrained Resnet18	Standard ResNet-18 Architecture	Standard	Standard	Adam	BCE
[140]	CNN	CNN Layers (2) + ReLU Activation + Pooling Layers (2) + FC Layers (2)	1 (rate=0.5)	NA	Adam	BCE
[76]	AE	AE with 8 Layers	NA	K-Means Clustering	NA	NA
[141]	CultureNet	Faster R-CNN + Modified ResNet50 + 5FC Layers	NA	Softmax	Adelta	Proposed Loss Function
[142]	DCNN	Proposed DCNN Architecture with Different Layers	NA	Decision Tree (DT)	Manual Optimization	NA
[143]	CNN	CNN Layers (2) + ReLU Activation + FC Layers (3)	4 (rate=0.2)	Softmax	NA	NA
[144]	SA-B3D with LSTM Model	CNN Layers (5) + LSTM Layers (1) + Pooling Layers (4) + FC Layers (1)	NA	Sigmoid	Adam	CE Proposed Loss Function
[74]	CNN	CNN Layers (3) + ReLU Activation + Pooling Layers (3) + FC Layers (1)	NA	SVM	SGD	NA
[145]	DENN	Proposed DENN Architecture with ReLU Activation + FC Layers (2)	NA	Sigmoid	mini-batch SGD	CCE
[146]	DNN	Proposed DNN with ReLU Activation + FC Layers (2)	(rate =0.2) (rate =0.4)	Sigmoid	Adam	BCE

REFERENCES

- [1] J. Kang, X. Han, J. Song, Z. Niu, and X. Li, "The identification of children with autism spectrum disorder by svm approach on eeg and eye-tracking data," *Computers in Biology and Medicine*, p. 103722, 2020.
- [2] B. S. Abrahams and D. H. Geschwind, "Advances in autism genetics: on the threshold of a new neurobiology," *Nature reviews genetics*, vol. 9, no. 5, pp. 341–355, 2008.
- [3] E. Stevens, D. R. Dixon, M. N. Novack, D. Granpeesheh, T. Smith, and E. Linstead, "Identification and analysis of behavioral phenotypes in autism spectrum disorder via unsupervised machine learning," *International journal of medical informatics*, vol. 129, pp. 29–36, 2019.
- [4] M. J. Maenner, K. A. Shaw, J. Baio *et al.*, "Prevalence of autism spectrum disorder among children aged 8 years—autism and developmental disabilities monitoring network, 11 sites, united states, 2016," *MMWR Surveillance Summaries*, vol. 69, no. 4, p. 1, 2020.
- [5] S. Yazdani, A. Capuano, M. Ghaziuddin, and C. Colombi, "Exclusion criteria used in early behavioral intervention studies for young children with autism spectrum disorder," *Brain Sciences*, vol. 10, no. 2, p. 99, 2020.
- [6] C. Andy and R. S. Masters, "Improving motor skill acquisition through analogy in children with autism spectrum disorders," *Psychology of Sport and Exercise*, vol. 41, pp. 63–69, 2019.
- [7] S. Mostafa, L. Tang, and F.-X. Wu, "Diagnosis of autism spectrum disorder based on eigenvalues of brain networks," *IEEE Access*, vol. 7, pp. 128 474–128 486, 2019.
- [8] A. Kazeminejad and R. C. Sotero, "Topological properties of resting-state fmri functional networks improve machine learning-based autism classification," *Frontiers in neuroscience*, vol. 12, p. 1018, 2019.
- [9] O. Dekhil, M. Ali, R. Haweel, Y. Elnakib, M. Ghazal, H. Hajjdiab, L. Fraiwan, A. Shalaby, A. Soliman, A. Mahmoud *et al.*, "A comprehensive framework for differentiating autism spectrum disorder from neurotypicals by fusing structural mri and resting state functional mri," in *Seminars in Pediatric Neurology*. Elsevier, 2020, p. 100805.
- [10] B. G. Travers, N. Adluru, C. Ennis, D. P. Tromp, D. Destiche, S. Doran, E. D. Bigler, N. Lange, J. E. Lainhart, and A. L. Alexander, "Diffusion tensor imaging in autism spectrum disorder: a review," *Autism Research*, vol. 5, no. 5, pp. 289–313, 2012.
- [11] J. Vicnesh, J. K. E. Wei, S. L. Oh, N. Arunkumar, E. W. Abdulhay, E. J. Ciaccio, U. R. Acharya *et al.*, "Autism spectrum disorder diagnostic system using hos bispectrum with eeg signals," *International Journal of Environmental Research and Public Health*, vol. 17, no. 3, p. 971, 2020.
- [12] D. Haputhanthri, G. Brihadiswaran, S. Gunathilaka, D. Meedeniya, S. Jayarathna, M. Jaime, and C. Harshaw, "Integration of facial thermography in eeg-based classification of asd," *International Journal of Automation and Computing*, vol. 17, pp. 1–18, 2020.
- [13] J. Kang, T. Zhou, J. Han, and X. Li, "Eeg-based multi-feature fusion assessment for autism," *Journal of Clinical Neuroscience*, vol. 56, pp. 101–107, 2018.
- [14] T. Sinha, M. V. Munot, and R. Sreemathy, "An efficient approach for detection of autism spectrum disorder using electroencephalography signal," *IETE Journal of Research*, pp. 1–9, 2019.
- [15] M. Sadeghi, R. Khosrowabadi, F. Bakouie, H. Mahdavi, C. Eslahchi, and H. Pourtemad, "Screening of autism based on task-free fmri using graph theoretical approach," *Psychiatry Research: Neuroimaging*, vol. 263, pp. 48–56, 2017.
- [16] A. Kazeminejad and R. C. Sotero, "Topological properties of resting-state fmri functional networks improve machine learning-based autism classification," *Frontiers in neuroscience*, vol. 12, p. 1018, 2019.
- [17] J. C. Siero, D. Hermes, H. Hoogduin, P. R. Luijten, N. F. Ramsey, and N. Petridou, "Bold matches neuronal activity at the mm scale: A combined 7 t fmri and ecog study in human sensorimotor cortex," *Neuroimage*, vol. 101, pp. 177–184, 2014.
- [18] L. Xu, Q. Hua, J. Yu, and J. Li, "Classification of autism spectrum disorder based on sample entropy of spontaneous functional near infrared spectroscopy signal," *Clinical Neurophysiology*, 2020.
- [19] R. G. Port, J. C. Edgar, M. Ku, L. Bloy, R. Murray, L. Blaskey, S. E. Levy, and T. P. Roberts, "Maturation of auditory neural processes in autism spectrum disorder—a longitudinal meg study," *NeuroImage: Clinical*, vol. 11, pp. 566–577, 2016.
- [20] R. C. Deo, "Machine learning in medicine," *Circulation*, vol. 132, no. 20, pp. 1920–1930, 2015.
- [21] I. Goodfellow, Y. Bengio, and A. Courville, *Deep learning*. MIT press, 2016.
- [22] J. Dolz, C. Desrosiers, L. Wang, J. Yuan, D. Shen, and I. B. Ayed, "Deep cnn ensembles and suggestive annotations for infant brain mri segmentation," *Computerized Medical Imaging and Graphics*, vol. 79, p. 101660, 2020.
- [23] N. Ghassemi, A. Shoeibi, and M. Rouhani, "Deep neural network with generative adversarial networks pre-training for brain tumor classification based on mr images," *Biomedical Signal Processing and Control*, vol. 57, p. 101678, 2020.
- [24] X. Li, N. C. Dvornek, X. Papademetris, J. Zhuang, L. H. Staib, P. Ventola, and J. S. Duncan, "2-channel convolutional 3d deep neural network (2cc3d) for fmri analysis: Asd classification and feature learning," in *2018 IEEE 15th International Symposium on Biomedical Imaging (ISBI 2018)*. IEEE, 2018, pp. 1252–1255.
- [25] Q. Delannoy, C.-H. Pham, C. Cazorla, C. Tor-Diez, G. Dollé, H. Meunier, N. Bednarek, R. Fablet, N. Passat, and F. Rousseau, "Segsrgan: Super-resolution and segmentation using generative adversarial networks—application to neonatal brain mri," *Computers in Biology and Medicine*, p. 103755, 2020.
- [26] R. Reed and R. J. MarksII, *Neural smithing: supervised learning in feedforward artificial neural networks*. MIT Press, 1999.
- [27] G. E. Hinton, T. J. Sejnowski, T. A. Poggio *et al.*, *Unsupervised learning: foundations of neural computation*. MIT press, 1999.
- [28] M. Wiering and M. Van Otterlo, *Reinforcement learning*. Springer, 2012, vol. 12.
- [29] J. Eldridge, A. E. Lane, M. Belkin, and S. Dennis, "Robust features for the automatic identification of autism spectrum disorder in children," *Journal of neurodevelopmental disorders*, vol. 6, no. 1, p. 12, 2014.
- [30] S. Bhat, U. R. Acharya, H. Adeli, G. M. Bairy, and A. Adeli, "Autism: cause factors, early diagnosis and therapies," *Reviews in the Neurosciences*, vol. 25, no. 6, pp. 841–850, 2014.
- [31] A. Dejman, A. Khadem, and A. Khorrami, "Exploring the disorders of brain effective connectivity network in asd: A case study using eeg, transfer entropy, and graph theory," in *2017 Iranian Conference on Electrical Engineering (ICEE)*. IEEE, 2017, pp. 8–13.
- [32] N. Ghassemi, A. Shoeibi, M. Rouhani, and H. Hosseini-Nejad, "Epileptic seizures detection in eeg signals using tqwt and ensemble learning," in *2019 9th International Conference on Computer and Knowledge Engineering (ICCKE)*. IEEE, 2019, pp. 403–408.
- [33] S. Bhat, U. R. Acharya, H. Adeli, G. M. Bairy, and A. Adeli, "Automated diagnosis of autism: in search of a mathematical marker," *Reviews in the Neurosciences*, vol. 25, no. 6, pp. 851–861, 2014.
- [34] F. Thabtah, "Machine learning in autistic spectrum disorder behavioral research: A review and ways forward," *Informatics for Health and Social Care*, vol. 44, no. 3, pp. 278–297, 2019.
- [35] D. Eman and A. W. Emanuel, "Machine learning classifiers for autism spectrum disorder: A review," in *2019 4th International Conference on Information Technology, Information Systems and Electrical Engineering (ICITISEE)*. IEEE, 2019, pp. 255–260.
- [36] "Autism brain imaging data exchange i," http://fcon_1000.projects.nitrc.org/indi/abide/abide_1.html, 2016.
- [37] "Abide preprocessed," <http://preprocessed-connectomes-project.org/abide/>.
- [38] N. Payakachat, J. M. Tilford, and W. J. Ungar, "National database for autism research (ndar): big data opportunities for health services research and health technology assessment," *Pharmacoeconomics*, vol. 34, no. 2, pp. 127–138, 2016.
- [39] M. Jenkinson, C. F. Beckmann, T. E. Behrens, M. W. Woolrich, and S. M. Smith, "Fsl," *Neuroimage*, vol. 62, no. 2, pp. 782–790, 2012.
- [40] V. Popescu, M. Battaglini, W. Hoogstrate, S. C. Verfaillie, I. Sluimer, R. A. van Schijndel, B. W. van Dijk, K. S. Cover, D. L. Knol, M. Jenkinson *et al.*, "Optimizing parameter choice for fsl-brain extraction tool (bet) on 3d t1 images in multiple sclerosis," *Neuroimage*, vol. 61, no. 4, pp. 1484–1494, 2012.
- [41] B. Fischl, "Freesurfer," *Neuroimage*, vol. 62, no. 2, pp. 774–781, 2012.
- [42] J. Ashburner, "Computational anatomy with the spm software," *Magnetic resonance imaging*, vol. 27, no. 8, pp. 1163–1174, 2009.
- [43] H. A. Jaber, H. K. Aljobouri, İ. Çankaya, O. M. Koçak, and O. Algin, "Preparing fmri data for postprocessing: Conversion modalities, pre-processing pipeline, and parametric and nonparametric approaches," *IEEE Access*, vol. 7, pp. 122 864–122 877, 2019.
- [44] M. Behroozi, M. R. Daliri, and H. Boyaci, "Statistical analysis methods for the fmri data," *Basic and Clinical Neuroscience*, vol. 2, no. 4, pp. 67–74, 2011.
- [45] B.-y. Park, K. Byeon, and H. Park, "Funp (fusion of neuroimaging preprocessing) pipelines: a fully automated preprocessing software for functional magnetic resonance imaging," *Frontiers in neuroinformatics*, vol. 13, p. 5, 2019.

- [46] J. A. Maldjian, P. J. Laurienti, R. A. Kraft, and J. H. Burdette, "An automated method for neuroanatomic and cytoarchitectonic atlas-based interrogation of fmri data sets," *Neuroimage*, vol. 19, no. 3, pp. 1233–1239, 2003.
- [47] N. Tzourio-Mazoyer, B. Landeau, D. Papathanassiou, F. Crivello, O. Etard, N. Delcroix, B. Mazoyer, and M. Joliot, "Automated anatomical labeling of activations in spm using a macroscopic anatomical parcellation of the mni mri single-subject brain," *Neuroimage*, vol. 15, no. 1, pp. 273–289, 2002.
- [48] S. B. Eickhoff, K. E. Stephan, H. Mohlberg, C. Grefkes, G. R. Fink, K. Amunts, and K. Zilles, "A new spm toolbox for combining probabilistic cytoarchitectonic maps and functional imaging data," *Neuroimage*, vol. 25, no. 4, pp. 1325–1335, 2005.
- [49] R. S. Desikan, F. Ségonne, B. Fischl, B. T. Quinn, B. C. Dickerson, D. Blacker, R. L. Buckner, A. M. Dale, R. P. Maguire, B. T. Hyman *et al.*, "An automated labeling system for subdividing the human cerebral cortex on mri scans into gyral based regions of interest," *Neuroimage*, vol. 31, no. 3, pp. 968–980, 2006.
- [50] J. Talairach, "Co-planar stereotaxic atlas of the human brain-3-dimensional proportional system," *An approach to cerebral imaging*, 1988.
- [51] N. U. Dosenbach, B. Nardos, A. L. Cohen, D. A. Fair, J. D. Power, J. A. Church, S. M. Nelson, G. S. Wig, A. C. Vogel, C. N. Lessov-Schlaggar *et al.*, "Prediction of individual brain maturity using fmri," *Science*, vol. 329, no. 5997, pp. 1358–1361, 2010.
- [52] R. C. Craddock, G. A. James, P. E. Holtzheimer III, X. P. Hu, and H. S. Mayberg, "A whole brain fmri atlas generated via spatially constrained spectral clustering," *Human brain mapping*, vol. 33, no. 8, pp. 1914–1928, 2012.
- [53] M. Kunda, S. Zhou, G. Gong, and H. Lu, "Improving multi-site autism classification based on site-dependence minimisation and second-order functional connectivity," *bioRxiv*, 2020.
- [54] "Abide preprocessed - functional preprocessing," <http://preprocessed-connectomes-project.org/abide/Pipelines.html>.
- [55] P. Bellec, C. Chu, F. Chouinard-Decorte, Y. Benhajali, D. S. Margulies, and R. C. Craddock, "The neuro bureau adhd-200 preprocessed repository," *Neuroimage*, vol. 144, pp. 275–286, 2017.
- [56] C. Yan and Y. Zang, "Dparsf: a matlab toolbox for" pipeline" data analysis of resting-state fmri," *Frontiers in systems neuroscience*, vol. 4, p. 13, 2010.
- [57] C. Craddock, S. Sikka, B. Cheung, R. Khanuja, S. S. Ghosh, C. Yan, Q. Li, D. Lurie, J. Vogelstein, R. Burns *et al.*, "Towards automated analysis of connectomes: The configurable pipeline for the analysis of connectomes (c-pac)," *Front Neuroinform*, vol. 42, 2013.
- [58] T. Xu, Z. Yang, L. Jiang, X.-X. Xing, and X.-N. Zuo, "A connectome computation system for discovery science of brain," *Science Bulletin*, vol. 60, no. 1, pp. 86–95, 2015.
- [59] N. C. Dvornek, D. Yang, P. Ventola, and J. S. Duncan, "Learning generalizable recurrent neural networks from small task-fmri datasets," in *International Conference on Medical Image Computing and Computer-Assisted Intervention*. Springer, 2018, pp. 329–337.
- [60] T. Eslami and F. Saeed, "Auto-asd-network: a technique based on deep learning and support vector machines for diagnosing autism spectrum disorder using fmri data," in *Proceedings of the 10th ACM International Conference on Bioinformatics, Computational Biology and Health Informatics*, 2019, pp. 646–651.
- [61] Z. Sherkatghanad, M. Akhondzadeh, S. Salari, M. Zomorodi-Moghadam, M. Abdar, U. R. Acharya, R. Khosrowabadi, and V. Salari, "Automated detection of autism spectrum disorder using a convolutional neural network," *Frontiers in Neuroscience*, vol. 13, 2019.
- [62] M. A. Aghdam, A. Sharifi, and M. M. Pedram, "Diagnosis of autism spectrum disorders in young children based on resting-state functional magnetic resonance imaging data using convolutional neural networks," *Journal of digital imaging*, vol. 32, no. 6, pp. 899–918, 2019.
- [63] O. Dekhil, H. Hajdiab, B. Ayinde, A. Shalaby, A. Switala, D. Sosnin, A. Elshamekh, M. Ghazal, R. Keynton, G. Barnes *et al.*, "Using resting state functional mri to build a personalized autism diagnosis system," in *2018 IEEE 15th International Symposium on Biomedical Imaging (ISBI 2018)*. IEEE, 2018, pp. 1381–1385.
- [64] F. Chollet, *Deep Learning mit Python und Keras: Das Praxis-Handbuch vom Entwickler der Keras-Bibliothek*. MITP-Verlags GmbH & Co. KG, 2018.
- [65] L. Zou, J. Zheng, C. Miao, M. J. Mckeown, and Z. J. Wang, "3d cnn based automatic diagnosis of attention deficit hyperactivity disorder using functional and structural mri," *IEEE Access*, vol. 5, pp. 23 626–23 636, 2017.
- [66] A. Radford, L. Metz, and S. Chintala, "Unsupervised representation learning with deep convolutional generative adversarial networks," *arXiv preprint arXiv:1511.06434*, 2015.
- [67] C. Doersch, "Tutorial on variational autoencoders," *arXiv preprint arXiv:1606.05908*, 2016.
- [68] Z. Che, S. Purushotham, K. Cho, D. Sontag, and Y. Liu, "Recurrent neural networks for multivariate time series with missing values," *Scientific reports*, vol. 8, no. 1, pp. 1–12, 2018.
- [69] J. Wang, Y. Yang, J. Mao, Z. Huang, C. Huang, and W. Xu, "Cnn-rnn: A unified framework for multi-label image classification," in *Proceedings of the IEEE conference on computer vision and pattern recognition*, 2016, pp. 2285–2294.
- [70] Y. Fan, X. Lu, D. Li, and Y. Liu, "Video-based emotion recognition using cnn-rnn and c3d hybrid networks," in *Proceedings of the 18th ACM International Conference on Multimodal Interaction*, 2016, pp. 445–450.
- [71] M. Chen, X. Shi, Y. Zhang, D. Wu, and M. Guizani, "Deep features learning for medical image analysis with convolutional autoencoder neural network," *IEEE Transactions on Big Data*, 2017.
- [72] M. I. U. Haque and D. Valles, "Facial expression recognition using dcnn and development of an ios app for children with asd to enhance communication abilities," in *2019 IEEE 10th Annual Ubiquitous Computing, Electronics & Mobile Communication Conference (UEMCON)*. IEEE, 2019, pp. 0476–0482.
- [73] M. I. U. Haque and D. Valles, "Facial expression recognition from different angles using dcnn for children with asd to identify emotions," in *2018 International Conference on Computational Science and Computational Intelligence (CSCI)*. IEEE, 2018, pp. 446–449.
- [74] N. M. Rad, S. M. Kia, C. Zarbo, T. van Laarhoven, G. Jurman, P. Venuti, E. Marchiori, and C. Furlanello, "Deep learning for automatic stereotypical motor movement detection using wearable sensors in autism spectrum disorders," *Signal Processing*, vol. 144, pp. 180–191, 2018.
- [75] C. Wu, S. Liaqat, S.-c. Cheung, C.-N. Chuah, and S. Ozonoff, "Predicting autism diagnosis using image with fixations and synthetic saccade patterns," in *2019 IEEE International Conference on Multimedia & Expo Workshops (ICMEW)*. IEEE, 2019, pp. 647–650.
- [76] M. Elbattah, R. Carette, G. Dequen, J.-L. Guérin, and F. Cilia, "Learning clusters in autism spectrum disorder: Image-based clustering of eye-tracking scanpaths with deep autoencoder," in *2019 41st Annual International Conference of the IEEE Engineering in Medicine and Biology Society (EMBC)*. IEEE, 2019, pp. 1417–1420.
- [77] X. Li, N. C. Dvornek, Y. Zhou, J. Zhuang, P. Ventola, and J. S. Duncan, "Efficient interpretation of deep learning models using graph structure and cooperative game theory: Application to asd biomarker discovery," in *International Conference on Information Processing in Medical Imaging*. Springer, 2019, pp. 718–730.
- [78] Y. Zhao, Q. Dong, S. Zhang, W. Zhang, H. Chen, X. Jiang, L. Guo, X. Hu, J. Han, and T. Liu, "Automatic recognition of fmri-derived functional networks using 3-d convolutional neural networks," *IEEE Transactions on Biomedical Engineering*, vol. 65, no. 9, pp. 1975–1984, 2017.
- [79] M. Leming, J. M. Górriz, and J. Suckling, "Ensemble deep learning on large, mixed-site fmri datasets in autism and other tasks," *arXiv preprint arXiv:2002.07874*, 2020.
- [80] X. Li, N. C. Dvornek, J. Zhuang, P. Ventola, and J. S. Duncan, "Brain biomarker interpretation in asd using deep learning and fmri," in *International Conference on Medical Image Computing and Computer-Assisted Intervention*. Springer, 2018, pp. 206–214.
- [81] M. Khosla, K. Jamison, A. Kuceyeski, and M. R. Sabuncu, "3d convolutional neural networks for classification of functional connectomes," in *Deep Learning in Medical Image Analysis and Multimodal Learning for Clinical Decision Support*. Springer, 2018, pp. 137–145.
- [82] F. Saeed, T. Eslami, V. Mirjalili, A. Fong, and A. Laird, "Asd-diagnet: A hybrid learning approach for detection of autism spectrum disorder using fmri data," *Frontiers in Neuroinformatics*, vol. 13, p. 70, 2019.
- [83] R. Anirudh and J. J. Thiagarajan, "Bootstrapping graph convolutional neural networks for autism spectrum disorder classification," in *ICASSP 2019-2019 IEEE International Conference on Acoustics, Speech and Signal Processing (ICASSP)*. IEEE, 2019, pp. 3197–3201.
- [84] C. J. Brown, J. Kawahara, and G. Hamarneh, "Connectome priors in deep neural networks to predict autism," in *2018 IEEE 15th International Symposium on Biomedical Imaging (ISBI 2018)*. IEEE, 2018, pp. 110–113.
- [85] D. Liao and H. Lu, "Classify autism and control based on deep learning and community structure on resting-state fmri," in *2018 Tenth Interna-*

- tional Conference on Advanced Computational Intelligence (ICACI)*. IEEE, 2018, pp. 289–294.
- [86] X. Yang, S. Sarraf, and N. Zhang, “Deep learning-based framework for autism functional mri image classification,” *Journal of the Arkansas Academy of Science*, vol. 72, no. 1, pp. 47–52, 2018.
- [87] X. Guo, K. C. Dominick, A. A. Minai, H. Li, C. A. Erickson, and L. J. Lu, “Diagnosing autism spectrum disorder from brain resting-state functional connectivity patterns using a deep neural network with a novel feature selection method,” *Frontiers in neuroscience*, vol. 11, p. 460, 2017.
- [88] M. Khosla, K. Jamison, A. Kuceyeski, and M. R. Sabuncu, “Ensemble learning with 3d convolutional neural networks for functional connectome-based prediction,” *Neuroimage*, vol. 199, pp. 651–662, 2019.
- [89] H. Choi, “Functional connectivity patterns of autism spectrum disorder identified by deep feature learning,” *arXiv preprint arXiv:1707.07932*, 2017.
- [90] N. C. Dvornek, P. Ventola, K. A. Pelphrey, and J. S. Duncan, “Identifying autism from resting-state fmri using long short-term memory networks,” in *International Workshop on Machine Learning in Medical Imaging*. Springer, 2017, pp. 362–370.
- [91] H. Lu, S. Liu, H. Wei, and J. Tu, “Multi-kernel fuzzy clustering based on auto-encoder for fmri functional network,” *Expert Systems with Applications*, p. 113513, 2020.
- [92] Z. Xiao, C. Wang, N. Jia, and J. Wu, “Sae-based classification of school-aged children with autism spectrum disorders using functional magnetic resonance imaging,” *Multimedia Tools and Applications*, vol. 77, no. 17, pp. 22 809–22 820, 2018.
- [93] N. C. Dvornek, X. Li, J. Zhuang, and J. S. Duncan, “Jointly discriminative and generative recurrent neural networks for learning from fmri,” in *International Workshop on Machine Learning in Medical Imaging*. Springer, 2019, pp. 382–390.
- [94] K. Niu, J. Guo, Y. Pan, X. Gao, X. Peng, N. Li, and H. Li, “Multichannel deep attention neural networks for the classification of autism spectrum disorder using neuroimaging and personal characteristic data,” *Complexity*, vol. 2020, 2020.
- [95] H. Li, N. A. Parikh, and L. He, “A novel transfer learning approach to enhance deep neural network classification of brain functional connectomes,” *Frontiers in neuroscience*, vol. 12, p. 491, 2018.
- [96] A. El Gazzar, L. Cerliani, G. van Wingen, and R. M. Thomas, “Simple 1-d convolutional networks for resting-state fmri based classification in autism,” in *2019 International Joint Conference on Neural Networks (IJCNN)*. IEEE, 2019, pp. 1–6.
- [97] M. R. Ahmed, Y. Zhang, Y. Liu, and H. Liao, “Single volume image generator and deep learning-based asd classification,” *IEEE Journal of Biomedical and Health Informatics*, 2020.
- [98] Y. Zhao, H. Dai, W. Zhang, F. Ge, and T. Liu, “Two-stage spatial temporal deep learning framework for functional brain network modeling,” in *2019 IEEE 16th International Symposium on Biomedical Imaging (ISBI 2019)*. IEEE, 2019, pp. 1576–1580.
- [99] B. Pugazhenthii, G. Senapathy, and M. Pavithra, “Identification of autism in mr brain images using deep learning networks,” in *2019 International Conference on Smart Structures and Systems (ICSSS)*. IEEE, 2019, pp. 1–7.
- [100] T. Eslami, J. S. Raiker, and F. Saeed, “Explainable and scalable machine-learning algorithms for detection of autism spectrum disorder using fmri data,” *arXiv preprint arXiv:2003.01541*, 2020.
- [101] K. Sairam, J. Naren, G. Vithya, and S. Srivathsan, “Computer aided system for autism spectrum disorder using deep learning methods,” *International Journal of Psychosocial Rehabilitation*, vol. 23, no. 01, 2019.
- [102] J. Dolz, C. Desrosiers, and I. B. Ayed, “3d fully convolutional networks for subcortical segmentation in mri: A large-scale study,” *NeuroImage*, vol. 170, pp. 456–470, 2018.
- [103] C. Wang, Z. Xiao, B. Wang, and J. Wu, “Identification of autism based on svm-rfe and stacked sparse auto-encoder,” *IEEE Access*, vol. 7, pp. 118 030–118 036, 2019.
- [104] Y. Zhao, F. Ge, S. Zhang, and T. Liu, “3d deep convolutional neural network revealed the value of brain network overlap in differentiating autism spectrum disorder from healthy controls,” in *International Conference on Medical Image Computing and Computer-Assisted Intervention*. Springer, 2018, pp. 172–180.
- [105] S. Parisot, S. I. Ktena, E. Ferrante, M. Lee, R. Guerrero, B. Glocker, and D. Rueckert, “Disease prediction using graph convolutional networks: Application to autism spectrum disorder and alzheimer’s disease,” *Medical image analysis*, vol. 48, pp. 117–130, 2018.
- [106] N. C. Dvornek, P. Ventola, and J. S. Duncan, “Combining phenotypic and resting-state fmri data for autism classification with recurrent neural networks,” in *2018 IEEE 15th International Symposium on Biomedical Imaging (ISBI 2018)*. IEEE, 2018, pp. 725–728.
- [107] A. S. Heinsfeld, A. R. Franco, R. C. Craddock, A. Buchweitz, and F. Meneguzzi, “Identification of autism spectrum disorder using deep learning and the abide dataset,” *NeuroImage: Clinical*, vol. 17, pp. 16–23, 2018.
- [108] X. Li, J. Hect, M. Thomason, and D. Zhu, “Interpreting age effects of human fetal brain from spontaneous fmri using deep 3d convolutional neural networks,” in *2020 IEEE 17th International Symposium on Biomedical Imaging (ISBI)*. IEEE, 2020, pp. 1424–1427.
- [109] M. A. Aghdam, A. Sharifi, and M. M. Pedram, “Combination of rs-fmri and smri data to discriminate autism spectrum disorders in young children using deep belief network,” *Journal of digital imaging*, vol. 31, no. 6, pp. 895–903, 2018.
- [110] C. Mellema, A. Treacher, K. Nguyen, and A. Montillo, “Multiple deep learning architectures achieve superior performance diagnosing autism spectrum disorder using features previously extracted from structural and functional mri,” in *2019 IEEE 16th International Symposium on Biomedical Imaging (ISBI 2019)*. IEEE, 2019, pp. 1891–1895.
- [111] M. Rakić, M. Cabezas, K. Kushibar, A. Oliver, and X. Lladó, “Improving the detection of autism spectrum disorder by combining structural and functional mri information,” *NeuroImage: Clinical*, vol. 25, p. 102181, 2020.
- [112] G. Li, M. Liu, Q. Sun, D. Shen, and L. Wang, “Early diagnosis of autism disease by multi-channel cnns,” in *International Workshop on Machine Learning in Medical Imaging*. Springer, 2018, pp. 303–309.
- [113] G. Li, M.-H. Chen, G. Li, D. Wu, Q. Sun, D. Shen, and L. Wang, “A preliminary volumetric mri study of amygdala and hippocampal subfields in autism during infancy,” in *2019 IEEE 16th International Symposium on Biomedical Imaging (ISBI 2019)*. IEEE, 2019, pp. 1052–1056.
- [114] M. Ismail, G. Barnes, M. Nitzken, A. Switala, A. Shalaby, E. Hosseini-Asl, M. Casanova, R. Keynton, A. Khalil, and A. El-Baz, “A new deep-learning approach for early detection of shape variations in autism using structural mri,” in *2017 IEEE International Conference on Image Processing (ICIP)*. IEEE, 2017, pp. 1057–1061.
- [115] Y. Kong, J. Gao, Y. Xu, Y. Pan, J. Wang, and J. Liu, “Classification of autism spectrum disorder by combining brain connectivity and deep neural network classifier,” *Neurocomputing*, vol. 324, pp. 63–68, 2019.
- [116] W. H. Pinaya, A. Mechelli, and J. R. Sato, “Using deep autoencoders to identify abnormal brain structural patterns in neuropsychiatric disorders: A large-scale multi-sample study,” *Human brain mapping*, vol. 40, no. 3, pp. 944–954, 2019.
- [117] S. J. Sujit, I. Coronado, A. Kamali, P. A. Narayana, and R. E. Gabr, “Automated image quality evaluation of structural brain mri using an ensemble of deep learning networks,” *Journal of Magnetic Resonance Imaging*, vol. 50, no. 4, pp. 1260–1267, 2019.
- [118] L. Henschel, S. Conjeti, S. Estrada, K. Diers, B. Fischl, and M. Reuter, “Fastsurfer—a fast and accurate deep learning based neuroimaging pipeline,” *NeuroImage*, p. 117012, 2020.
- [119] H. Shahamat and M. S. Abadeh, “Brain mri analysis using a deep learning based evolutionary approach,” *Neural Networks*, 2020.
- [120] J. E. Iglesias, G. Lerma-Usabiaga, L. C. Garcia-Peraza-Herrera, S. Martinez, and P. M. Paz-Alonso, “Retrospective head motion estimation in structural brain mri with 3d cnns,” in *International Conference on Medical Image Computing and Computer-Assisted Intervention*. Springer, 2017, pp. 314–322.
- [121] K. Byeon, J. Kwon, J. Hong, and H. Park, “Artificial neural network inspired by neuroimaging connectivity: Application in autism spectrum disorder,” in *2020 IEEE International Conference on Big Data and Smart Computing (BigComp)*. IEEE, 2020, pp. 575–578.
- [122] L. Xu, Y. Liu, J. Yu, X. Li, X. Yu, H. Cheng, and J. Li, “Characterizing autism spectrum disorder by deep learning spontaneous brain activity from functional near-infrared spectroscopy,” *Journal of Neuroscience Methods*, vol. 331, p. 108538, 2020.
- [123] L. Xu, X. Geng, X. He, J. Li, and J. Yu, “Prediction in autism by deep learning short-time spontaneous hemodynamic fluctuations,” *Frontiers in Neuroscience*, vol. 13, 2019.
- [124] B. Thyreau and Y. Taki, “Learning a cortical parcellation of the brain robust to the mri segmentation with convolutional neural networks,” *Medical Image Analysis*, vol. 61, p. 101639, 2020.
- [125] R. M. Thomas, S. Gallo, L. Cerliani, P. Zhutovsky, A. El-Gazzar, and G. van Wingen, “Classifying autism spectrum disorder using the temporal statistics of resting-state functional mri data with 3d

- convolutional neural networks,” *Frontiers in Psychiatry*, vol. 11, p. 440, 2020.
- [126] A. El-Gazzar, M. Quaak, L. Cerliani, P. Bloem, G. van Wingen, and R. M. Thomas, “A hybrid 3dcnn and 3dc-lstm based model for 4d spatio-temporal fmri data: An abide autism classification study,” in *OR 2.0 Context-Aware Operating Theaters and Machine Learning in Clinical Neuroimaging*. Springer, 2019, pp. 95–102.
- [127] S. Mostafa, W. Yin, and F.-X. Wu, “Autoencoder based methods for diagnosis of autism spectrum disorder,” in *International Conference on Computational Advances in Bio and Medical Sciences*. Springer, 2019, pp. 39–51.
- [128] Z. Jiao, H. Li, and Y. Fan, “Improving diagnosis of autism spectrum disorder and disentangling its heterogeneous functional connectivity patterns using capsule networks,” in *2020 IEEE 17th International Symposium on Biomedical Imaging (ISBI)*. IEEE, 2020, pp. 1331–1334.
- [129] J. Xie, L. Wang, P. Webster, Y. Yao, J. Sun, S. Wang, and H. Zhou, “A two-stream end-to-end deep learning network for recognizing atypical visual attention in autism spectrum disorder,” *arXiv preprint arXiv:1911.11393*, 2019.
- [130] S. Sadiq, M. Castellanos, J. Moffitt, M.-L. Shyu, L. Perry, and D. Messinger, “Deep learning based multimedia data mining for autism spectrum disorder (asd) diagnosis,” in *2019 International Conference on Data Mining Workshops (ICDMW)*. IEEE, 2019, pp. 847–854.
- [131] Y. Tao and M.-L. Shyu, “Sp-asdnet: Cnn-lstm based asd classification model using observer scanpaths,” in *2019 IEEE International Conference on Multimedia & Expo Workshops (ICMEW)*. IEEE, 2019, pp. 641–646.
- [132] J. R. H. Lee and A. Wong, “Timeconvnets: A deep time windowed convolution neural network design for real-time video facial expression recognition,” in *2020 17th Conference on Computer and Robot Vision (CRV)*. IEEE, 2020, pp. 9–16.
- [133] A. Vijayan, S. Janmasree, C. Keerthana, and L. B. Sylva, “A framework for intelligent learning assistant platform based on cognitive computing for children with autism spectrum disorder,” in *2018 International CET Conference on Control, Communication, and Computing (IC4)*. IEEE, 2018, pp. 361–365.
- [134] A. Di Nuovo, D. Conti, G. Trubia, S. Buono, and S. Di Nuovo, “Deep learning systems for estimating visual attention in robot-assisted therapy of children with autism and intellectual disability,” *Robotics*, vol. 7, no. 2, p. 25, 2018.
- [135] N. M. Rad, S. M. Kia, C. Zarbo, T. van Laarhoven, G. Jurman, P. Venuti, E. Marchiori, and C. Furlanello, “Deep learning for automatic stereotypical motor movement detection using wearable sensors in autism spectrum disorders,” *Signal Processing*, vol. 144, pp. 180–191, 2018.
- [136] S. Jaiswal, M. F. Valstar, A. Gillott, and D. Daley, “Automatic detection of adhd and asd from expressive behaviour in rgb-d data,” in *2017 12th IEEE International Conference on Automatic Face & Gesture Recognition (FG 2017)*. IEEE, 2017, pp. 762–769.
- [137] Y.-S. Liu, C.-P. Chen, S. S.-F. Gau, and C.-C. Lee, “Learning lexical coherence representation using lstm forget gate for children with autism spectrum disorder during story-telling,” in *2018 IEEE International Conference on Acoustics, Speech and Signal Processing (ICASSP)*. IEEE, 2018, pp. 6029–6033.
- [138] J. Li, Y. Zhong, J. Han, G. Ouyang, X. Li, and H. Liu, “Classifying asd children with lstm based on raw videos,” *Neurocomputing*, 2019.
- [139] W. Wei, Z. Liu, L. Huang, A. Nebout, and O. Le Meur, “Saliency prediction via multi-level features and deep supervision for children with autism spectrum disorder,” in *2019 IEEE International Conference on Multimedia & Expo Workshops (ICMEW)*. IEEE, 2019, pp. 621–624.
- [140] S. Raj and S. Masood, “Analysis and detection of autism spectrum disorder using machine learning techniques,” *Procedia Computer Science*, vol. 167, pp. 994–1004, 2020.
- [141] O. Rudovic, Y. Utsumi, J. Lee, J. Hernandez, E. C. Ferrer, B. Schuller, and R. W. Picard, “Culturenet: A deep learning approach for engagement intensity estimation from face images of children with autism,” in *2018 IEEE/RSJ International Conference on Intelligent Robots and Systems (IROS)*. IEEE, 2018, pp. 339–346.
- [142] A. Cook, B. Mandal, D. Berry, and M. Johnson, “Towards automatic screening of typical and atypical behaviors in children with autism,” in *2019 IEEE International Conference on Data Science and Advanced Analytics (DSAA)*. IEEE, 2019, pp. 504–510.
- [143] H. Javed and C. H. Park, “Behavior-based risk detection of autism spectrum disorder through child-robot interaction,” in *Companion of the 2020 ACM/IEEE International Conference on Human-Robot Interaction*, 2020, pp. 275–277.
- [144] K. Sun, L. Li, L. Li, N. He, and J. Zhu, “Spatial attentional bilinear 3d convolutional network for video-based autism spectrum disorder detection,” in *ICASSP 2020-2020 IEEE International Conference on Acoustics, Speech and Signal Processing (ICASSP)*. IEEE, 2020, pp. 3387–3391.
- [145] H. Wang, L. Li, L. Chi, and Z. Zhao, “Autism screening using deep embedding representation,” in *International Conference on Computational Science*. Springer, 2019, pp. 160–173.
- [146] M. F. Misman, A. A. Samah, F. A. Ezudin, H. A. Majid, Z. A. Shah, H. Hashim, and M. F. Harun, “Classification of adults with autism spectrum disorder using deep neural network,” in *2019 1st International Conference on Artificial Intelligence and Data Sciences (AiDAS)*. IEEE, 2019, pp. 29–34.